

THE STRUCTURAL CHEMISTRY OF SOME
PEROXOVANADATE(V) COMPLEXES

by

RALPH EDWARD DREW

B.Sc., Simon Fraser University, 1971

A THESIS SUBMITTED IN PARTIAL FULFILMENT
OF THE REQUIREMENTS FOR THE DEGREE OF
MASTER OF SCIENCE
in the Department
of
Chemistry

© RALPH EDWARD DREW, 1973

SIMON FRASER UNIVERSITY

April , 1973

APPROVAL

Name: Ralph Edward Drew
Degree: Master of Science
Title of Thesis: The Structural Chemistry Of Some
Peroxovanadate(V) Complexes.

Examining Committee:

Chairman: D.Sutton

F.W.B.Einstein
Senior Supervisor

L.K.Peterson

K.N.Slessor

A.Curzon
Department of Physics

Date Approved: March 20th 1973

PARTIAL COPYRIGHT LICENSE

I hereby grant to Simon Fraser University the right to loan my thesis or dissertation (the title of which is shown below) to users of the Simon Fraser University Library, and to make partial or single copies only for such users or in response to a request from the library of any other university, or other educational institution, on its own behalf or for one of its users. I further agree that permission for multiple copying of this thesis for scholarly purposes may be granted by me or the Dean of Graduate Studies. It is understood that copying or publication of this thesis for financial gain shall not be allowed without my written permission.

Title of Thesis/Dissertation:

The Structural Chemistry of Some
Peroxovanadate(V) Complexes.

Author:

(signature)

Ralph Edward Drew

(name)

March 14, 1973.

(date)

ABSTRACT

The crystal structures of two peroxovanadate(V) complexes, $\text{NH}_4[\text{VO}(\text{O}_2)_2(\text{NH}_3)]$ (I) and $\text{NH}_4[\text{VO}(\text{O}_2)(\text{H}_2\text{O})(\text{C}_5\text{H}_3\text{N}(\text{COO})_2)] \cdot x\text{H}_2\text{O}$ ($x \approx 1.3$) (II), were determined from three-dimensional x-ray diffraction intensity data collected by counter methods on a computer controlled Picker four-circle diffractometer. The data for (II) was collected at -100°C by using a Joule-Thomson low temperature device. The phase problem was solved using the Patterson synthesis for (I) and Symbolic Addition Procedures for (II). Refinement by full-matrix least-squares methods gave conventional R values of 3.1% for both the 566 reflections observed for (I) and the 1331 reflections observed for (II).

The compound (I) crystallizes in the orthorhombic space group P_{2121} with four formula units in a cell of dimensions $a = 8.370(2)$, $b = 6.877(1)$, and $c = 9.244(2)$ Å. The coordination of the vanadium atom can best be described in terms of a pentagonal pyramid, the four oxygens of the two peroxy groups and the nitrogen atom of the NH_3 group forming the distorted base of the pyramid, while the vanadyl oxygen atom occupies the apical position. Each ion has crystallographic mirror symmetry, the peroxy groups being the only nonhydrogen atoms lying off the mirror plane. Analysis of the motion of the anion as a rigid body yields bond lengths of 1.883(3) and 1.882(3) Å for the $\text{V}-\text{O}_{\text{peroxy}}$ bonds, 1.606(3) Å for the $\text{V}=\text{O}$ bond, 2.110(4) Å for the $\text{V}-\text{NH}_3$ bond, and 1.472(4) Å for the $\text{O}-\text{O}$ bond.

The compound (II) crystallizes in the monoclinic space group $C_{2/c}$ with eight formula units in a cell having lattice constants $a = 11.307(2)$, $b = 25.490(5)$, $c = 8.316(2)$ Å and $\beta = 96.90(1)^\circ$ at $-100(2)^\circ\text{C}$. The structure is comprised of two crystallographically different ammonium ions, one lying on a two-fold axis and the other on a center of symmetry, and a vanadium based anion. These ions are held together by both electrostatic forces and extensive hydrogen bonding. The vanadium atom environment is a seven coordinate distorted pentagonal bipyramid, with a vanadyl oxygen atom and a water molecule at the apices and a peroxy group, the nitrogen atom from the pyridine ring and one oxygen atom from each carboxylate group forming an approximate pentagonal plane. The vanadium atom is displaced 0.25 Å from the equatorial 'plane' towards the vanadyl oxygen atom. Interatomic distances within the anion are 1.870(2) and 1.872(2) Å for the V-O_{peroxy} bonds, 1.579(2) Å for the V=O bond, 2.053(2) and 2.064(2) Å for the V-O_{carboxylate} bonds, 2.211(2) Å for the V-O_{water} distance, 2.088(2) Å for the V-N distance, and 1.441(2) Å for the O-O bond.

To Carol and Ryan

ACKNOWLEDGEMENTS

I would like to express my gratitude to my Research Director, Dr. F.W.B.Einstein, for his helpful guidance and advice throughout the period of this work.

My sincere thanks are also extended to:

Dr. R.D.G.Jones and Dr. M.M.Gilbert for their interest and helpful discussions relating to this work;

All those faculty, staff and fellow students who entered into the many hours of sometimes provocative discussion in room C8046;

And my wife, Carol, who has had to put up with many 'lonely' evenings and weekends while I was at the University.

The National Research Council of Canada is also gratefully acknowledged for the financial support given to the crystallographic laboratory.

TABLE OF CONTENTS

	Page
LIST OF TABLES.....	viii
LIST OF FIGURES.....	ix
LIST OF ABBREVIATIONS.....	x
1. Introduction.....	1
2. Experimental.....	5
2.1. Preparative Procedures.....	5
2.2. Preliminary Examination and Photography.....	6
2.3. Diffractometry.....	10
3. Analysis of the Diffraction Data.....	15
3.1. Structure Determination For $\text{NH}_4[\text{VO}(\text{O}_2)_2(\text{NH}_3)]$	15
3.2. Structure Determination For $\text{NH}_4[\text{VO}(\text{O}_2)(\text{H}_2\text{O})(\text{C}_5\text{H}_3\text{N}(\text{COO})_2)] \cdot x\text{H}_2\text{O}$ ($x \approx 1.3$).....	26
4. Discussion of the Results.....	42
4.1. $\text{NH}_4[\text{VO}(\text{O}_2)_2(\text{NH}_3)]$	42
4.2. $\text{NH}_4[\text{VO}(\text{O}_2)(\text{H}_2\text{O})(\text{C}_5\text{H}_3\text{N}(\text{COO})_2)] \cdot x\text{H}_2\text{O}$ ($x \approx 1.3$).....	46
4.3. Sequel.....	53
APPENDIX A.....	54
APPENDIX B.....	64
APPENDIX C.....	66
REFERENCES.....	68

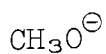
LIST OF TABLES

Table	Page
I Crystal Data.....	8
II Final Positional and Thermal Parameters For $\text{NH}_4[\text{VO}(\text{O}_2)_2(\text{NH}_3)]$	19
III Interatomic Distances and Angles For $\text{NH}_4[\text{VO}(\text{O}_2)_2(\text{NH}_3)]$.	20
IV Mean Plane For $\text{NH}_4[\text{VO}(\text{O}_2)_2(\text{NH}_3)]$	22
V Eigenvectors and Direction Cosines From The Rigid-Body Analysis For $\text{NH}_4[\text{VO}(\text{O}_2)_2(\text{NH}_3)]$	23
VI Final Positional and Thermal Parameters For $\text{NH}_4[\text{VO}(\text{O}_2)(\text{H}_2\text{O})(\text{C}_5\text{H}_3\text{N}(\text{COO})_2)] \cdot x\text{H}_2\text{O}$ ($x \approx 1.3$).....	31
VII Interatomic Distances and Angles For $\text{NH}_4[\text{VO}(\text{O}_2)(\text{H}_2\text{O})(\text{C}_5\text{H}_3\text{N}(\text{COO})_2)] \cdot x\text{H}_2\text{O}$ ($x \approx 1.3$).....	33
VIII Least-Squares Mean Planes For $\text{NH}_4[\text{VO}(\text{O}_2)(\text{H}_2\text{O})(\text{C}_5\text{H}_3\text{N}(\text{COO})_2)] \cdot x\text{H}_2\text{O}$ ($x \approx 1.3$).....	37
IX Angles Between The Least-Squares Mean Planes For $\text{NH}_4[\text{VO}(\text{O}_2)(\text{H}_2\text{O})(\text{C}_5\text{H}_3\text{N}(\text{COO})_2)] \cdot x\text{H}_2\text{O}$ ($x \approx 1.3$).....	38
X Eigenvectors and Direction Cosines From The Rigid-Body Analysis For $\text{NH}_4[\text{VO}(\text{O}_2)(\text{H}_2\text{O})(\text{C}_5\text{H}_3\text{N}(\text{COO})_2)] \cdot x\text{H}_2\text{O}$ ($x \approx 1.3$).....	39
XI Comparison Between The Corresponding Bond Lengths And Angles For The Compounds $\text{NH}_4[\text{VO}(\text{O}_2)(\text{H}_2\text{O})(\text{C}_5\text{H}_3\text{N}(\text{COO})_2)] \cdot x\text{H}_2\text{O}$ ($x \approx 1.3$), $\text{K}_2[\text{O}(\text{Ti}(\text{O}_2)(\text{H}_2\text{O})(\text{C}_5\text{H}_3\text{N}(\text{COO})_2))_2] \cdot 3\text{H}_2\text{O}$, Dipicolinic Acid, Calcium Dipicolinate, And Strontium Dipicolinate.....	51

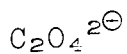
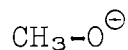
LIST OF FIGURES

Figure	Page
1 The $[\text{VO}(\text{O}_2)_2(\text{NH}_3)]^\ominus$ Anion.....	24
2 Stereoscopic Crystal Packing Diagram For $\text{NH}_4[\text{VO}(\text{O}_2)_2(\text{NH}_3)]$	25
3 The $[\text{VO}(\text{O}_2)(\text{H}_2\text{O})(\text{C}_5\text{H}_3\text{N}(\text{COO})_2)]^\ominus$ Anion.....	40
4 A Projection Down The <u>c</u> -Axis Of The Unit Cell For $\text{NH}_4[\text{VO}(\text{O}_2)(\text{H}_2\text{O})(\text{C}_5\text{H}_3\text{N}(\text{COO})_2)] \cdot x\text{H}_2\text{O}$ ($x \approx 1.3$).....	41

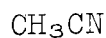
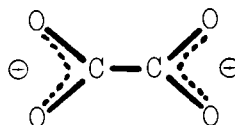
LIST OF ABBREVIATIONS



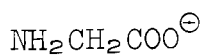
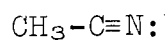
methoxide



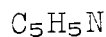
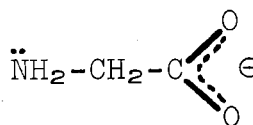
oxalato



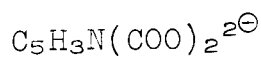
acetonitrile



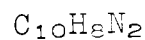
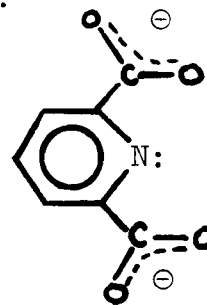
glycinato



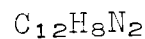
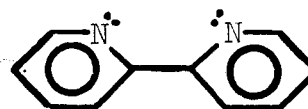
pyridine



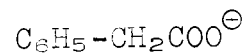
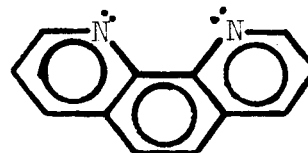
pyridine-2,6-dicarboxylato



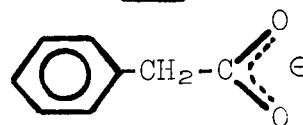
2,2'-bipyridyl



o-phenanthroline



phenylacetato



The numbered atoms used in the text refer to Figures 1 and 3.

CHAPTER 1

INTRODUCTION

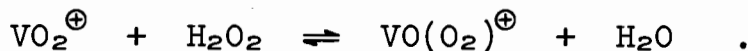
The chemistry of the transition metal peroxy complexes has been extensively investigated¹, but, prior to the last decade, relatively few structural studies had been carried out. In the last ten years, however, the number of structure determinations has increased markedly as computer hardware and software became more accessible to crystallographers, but the majority of the structural work on the transition metal peroxy complexes has been limited to those of chromium, molybdenum and cobalt.

The earliest structural work known for the peroxovanadate(V) compounds was the demonstration of the isomorphism of the compounds $K_3[M^v(O_2)_4]$ ($M^v = V, Cr, Nb$ or Ta) by x-ray powder photographic methods²; both the chromium³ and niobium⁴ compounds having been shown to have a quasi-dodecahedral structure. Reference has recently been made⁵ to the structure determination of $(NH_4)_3[V(O_2)_4]$, but information is presently minimal. The analogy between these tetraperoxo complexes has prompted recent work⁶ on the synthesis of triperoxovanadates which have been proposed to have possible eight coordination of the metal similar to that observed in the peroxoniobate(V) compounds $K[Nb(O_2)_3(C_{12}H_8N_2)] \cdot 3H_2O$ ⁷, $K[Nb(O_2)_3(C_{12}H_8N_2)] \cdot 3H_2O \cdot H_2O_2$ ⁷, $(NH_4)_3[Nb(O_2)_2(C_2O_4)_2] \cdot H_2O$ ⁸, and $KMg[Nb(O_2)_4] \cdot 7H_2O$ ⁴, in which the niobium was shown to have dodecahedral coordination.

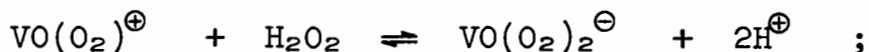
The recent elucidation of the structures of $(\text{NH}_4)_3[\text{V}(\text{O}_2)_4]$ ⁵ and $(\text{NH}_4)_4[\text{O}(\text{VO}(\text{O}_2)_2)_2]$ ⁵ can be considered as representing the first structural data on the peroxovanadate(V) complexes to appear in the literature. The dinuclear $[\text{O}(\text{VO}(\text{O}_2)_2)_2]$ ^{4⊖} anion was demonstrated⁵ to have distorted pentagonal bipyramidal coordination geometry around each vanadium atom, somewhat analogous to the anions $[\text{O}(\text{MoO}(\text{O}_2)_2(\text{H}_2\text{O}))_2]$ ^{2⊖}⁹⁻¹¹ and $[\text{O}(\text{WO}(\text{O}_2)_2(\text{H}_2\text{O}))_2]$ ^{2⊖}¹², and similar to that observed for the mononuclear oxodiperoxochromium(VI) complexes $[\text{CrO}(\text{O}_2)_2(\text{C}_5\text{H}_5\text{N})]$ ¹³, $[\text{CrO}(\text{O}_2)_2(\text{C}_{10}\text{H}_8\text{N}_2)]$ ¹⁴, and $[\text{CrO}(\text{O}_2)_2(\text{C}_{12}\text{H}_8\text{N}_2)]$ ¹⁵. Since vanadium(V) and chromium(VI) are both d⁰ systems, then it is not surprising that there are some structural similarities. On the other hand, there are also some interesting differences which so far have not been observed for the peroxochromium(VI) complexes, e.g. the formation of the dinuclear-diperoxo species and the mononuclear-monoperoxo species. Thus, it follows that structural data on the peroxovanadate(V) complexes will not only provide a unique opportunity for comparison with the already characterized stereochemistry of the peroxochromium(VI) complexes, but will also be useful in directing future synthetic work on other transition metal peroxy complexes.

At hydrogen ion concentrations above 0.01M, vanadium(V) in low concentration exists only as the VO_2^{\oplus} cation¹⁶⁻¹⁸. With hydrogen peroxide in acid solution, VO_2^{\oplus} forms the well characterized red 1:1 monoperoxo- and yellow 2:1 diperoxovanadates, the formation of the latter being favoured in high hydrogen peroxide concentration and/or low hydrogen ion concentration. The formation

of the red species $\text{VO}(\text{O}_2)^{\oplus}$ is independent of the nature or concentration of acid and involves¹⁹ :



It has been shown^{20,21} that the red and yellow forms, $\text{VO}(\text{O}_2)_2^{\ominus}$, are related in perchloric acid as :



which eliminates the previous formulation of the yellow species as e.g. $\text{V}(\text{O})_2(\text{O}_2)_2^{3\ominus}$ ^{1,22,23}. Thus, the 2:1 species $\text{VO}(\text{O}_2)_2^{\ominus}$ has acidic properties, and the observed decrease in pH when H_2O_2 is added to a metavanadate is explained; in the presence of excess metavanadate, polymerization will tend to occur¹. With increasing alkalinity this diperoxo anion is converted to the 3:1 species $\text{VO}(\text{O}_2)_3^{3\ominus}$, which is stable only in the presence of excess hydrogen peroxide. Similarly, the 4:1 species $\text{V}(\text{O}_2)_4^{3\ominus}$ is favoured by very alkaline media and high hydrogen peroxide concentrations¹. Thus, the number of peroxy groups per vanadium atom increases with alkalinity and hydrogen peroxide concentration. The 2:1 species $[\text{O}(\text{VO}(\text{O}_2)_2)_2]^{4\ominus}$ is favoured²⁴ by high concentrations of vanadium and is converted to the 3:1 species $[\text{VO}(\text{O}_2)_3]^{3\ominus}$ by high concentrations of hydrogen peroxide. Thus, increasing the concentration of hydrogen peroxide decreases the degree of polymerization.

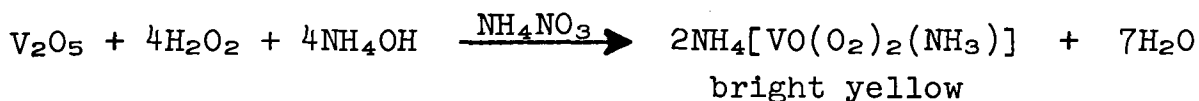
To study the stereochemistry of the above 2:1 and 1:1 peroxo-vanadate(V) species, the compounds $\text{NH}_4[\text{VO}(\text{O}_2)_2(\text{NH}_3)]$ and $\text{NH}_4[\text{VO}(\text{O}_2)(\text{H}_2\text{O})(\text{C}_5\text{H}_3\text{N}(\text{COO})_2)]$ ^{25,26} were chosen for x-ray structural analysis. Unlike the peroxochromium(VI) complexes, these compounds were quite stable and crystallized as single

crystals which were more than suitable for x-ray diffraction studies. In addition, since the crystal structure of $K_2[O(Ti(O_2)(H_2O)(C_5H_3N(COO)_2))_2].3H_2O$ had recently been determined²⁷, there was the advantage of being able to compare a peroxovanadium(V) species with a peroxotitanium(IV) species, again both being d^0 systems. Attempts to obtain single crystals of $K[VO(O_2)_2(H_2O)]$ ^{28,29} and $NH_4[VO(O_2)_2(H_2O)]$ were unsuccessful. Powder photographs have shown³⁰, however, that these two compounds are isomorphous, and very similar to $NH_4[VO(O_2)_2(NH_3)]$.

CHAPTER 2
EXPERIMENTAL

2.1. Preparative Procedures.

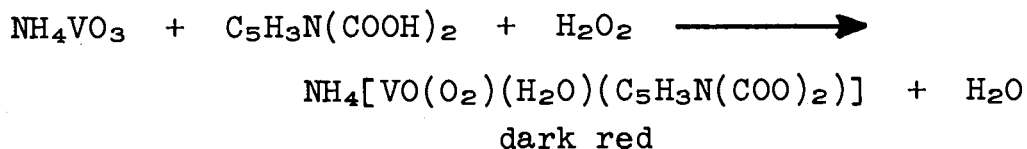
The preparation of ammonium oxodiperoxoamminevanadate(V), $\text{NH}_4[\text{VO}(\text{O}_2)_2(\text{NH}_3)]$ (I), was based on previous equilibria studies²⁰⁻²² involving the formation of the $\text{VO}(\text{O}_2)_2^\ominus$ anion, and procedures^{28,29} used in the preparation of compounds containing the $[\text{VO}(\text{O}_2)_2(\text{H}_2\text{O})]^\ominus$ anion :



The procedure involved dissolving divanadium pentoxide, V_2O_5 (1.82g, 0.01 mole), in 30% hydrogen peroxide (50ml) to obtain a deep red solution, i.e. the 1:1 species $\text{VO}(\text{O}_2)^\oplus$. To this solution ammonium nitrate (1.60g, 0.02 mole) was added, immediately followed by concentrated ammonium hydroxide, which was added dropwise until a bright yellow solution was obtained, i.e. the 2:1 species $\text{VO}(\text{O}_2)_2^\ominus$. This solution was allowed to stand for approximately twelve (12) hours, after which the mother liquor was decanted from the bright yellow crystals which had formed. These crystals were quite stable in air at room temperature, and showed no decomposition after many months. A melting point could not be obtained due to a gradual decomposition upon heating.

The preparation of ammonium oxoperoxo(pyridine-2,6-dicarboxylato) vanadate(V) hydrate, $\text{NH}_4[\text{VO}(\text{O}_2)(\text{H}_2\text{O})(\text{C}_5\text{H}_3\text{N}(\text{COO})_2)] \cdot x\text{H}_2\text{O}$ ($x \approx 1.3$) (II), was first reported by H. Hartkamp^{25,26}, and it was this

procedure which was utilized here. The method involved the reaction of ammonium vanadate, NH_4VO_3 , pyridine-2,6-dicarboxylic acid, and hydrogen peroxide in the ratio 1:1:1 to give a dark red solution from which large dark red crystals quickly formed :



As was the case for the diperoxo species, these crystals were stable in air at room temperature, but decomposed upon heating.

2.2. Preliminary Examination And Photography.

Samples of the prepared crystals were examined under a polarizing microscope, as a first indication to crystal quality, prior to selecting and mounting a crystal on a glass fibre for photography. Once a crystal was selected and mounted, it was aligned on a two-circle Nonius Optical Goniostat and then studied on the Weissenberg and precession cameras to determine its quality, setting, cell dimensions, Laue symmetry and possible space groups.

From the small crystals of (I), a needle-shaped crystal was selected and cleaved to maximum dimensions 0.13 x 0.40 x 0.13 mm in the directions a, b and c, respectively. This single crystal was mounted with the longest dimension parallel to the rotation axis and was used for both the preliminary photography and the data collection. Weissenberg photographs of the h0l - h3l zones and precession photographs of the hk0 and 0kl zones, using Cu $K\alpha$ radiation, showed absences for 0kl, k+1=2n+1, and for hk0, h=2n+1.

This, combined with the Laue group mmm , indicated either the space group P_{212121} or P_{212} . The former was subsequently chosen as providing an adequate model.

From the large crystals of (II), a crystal fragment of maximum dimensions $0.46 \times 0.25 \times 0.34$ mm in the directions a , b and c , respectively, was selected and mounted with the longest dimension approximately parallel to the rotation axis. This crystal was used for data collection; other larger crystals were used for the preliminary photography. Weissenberg photographs of the $0kl - 3kl$ zones and precession photographs of the $hk0 - hk1$ and $h0l - h2l$ zones using Cu $K\alpha$ radiation, showed absences for hkl , $h+k=2n+1$, and $h0l$, $l=2n+1$ ($h=2n+1$). This, combined with the Laue symmetry $2/m$, indicated the space group as either C_c or $C_{2/c}$; the latter centrosymmetric space group was subsequently selected as providing the most satisfactory model.

The densities of both (I) and (II) were measured using a Berman density balance, and, with the cell dimensions determined from the photographs, the number of molecules per unit cell (Z) was calculated from the formula :

$$Z = \frac{\rho NV}{M} \quad (2.1)$$

where ρ = the measured density of the compound

N = Avogadro's number (6.023×10^{23})

V = the unit cell volume (in cm^3) of the compound

M = the gram formula weight of the compound

A complete summary of the crystal data for both compounds is included for comparison in Table I.

Table I : Crystal Data

	I	II
STRUCTURE :	I	II
FORMULA :	$\text{NH}_4[\text{VO}(\text{O}_2)_2(\text{NH}_3)]$	$\text{NH}_4[\text{VO}(\text{O}_2)(\text{H}_2\text{O})-(\text{C}_5\text{H}_3\text{N}(\text{COO})_2)] \cdot x\text{H}_2\text{O}$
FORMULA WEIGHT :	166.0	323.6
COLOUR :	bright yellow	dark red
ZONES PHOTOGRAPHED :		
Weissenberg (Cu $K\alpha$) :	$\underline{h01-h31}$	$\underline{0k1-3k1}$
Precession (Cu $K\alpha$) :	$\underline{hk0}, \underline{0k1}$	$\underline{hk0-hk1}, \underline{h01-h21}$
SYSTEMATIC ABSENCES :	$\underline{0k1}, \underline{k+1=2n+1}$ $\underline{hk0}, \underline{h=2n+1}$	$\underline{hkl}, \underline{h+k=2n+1}$ $\underline{h01}, \underline{1=2n+1} (\underline{h=2n+1})$
LAUE SYMMETRY :	mmm	2/m
CRYSTAL SYSTEM :	orthorhombic	monoclinic
SPACE GROUP :	P_{222}	C_2/c
DIFFRACTOMETRY :		
Crystal Dimensions :	0.13x0.40x0.13mm	0.46x0.25x0.34mm
Mounting Axis :	\underline{b}	\underline{a}
Accurate Cell Dimensions :		
no. reflections used	10	17
range in 2θ	$50^\circ < 2\theta \leq 60^\circ$	$38^\circ < 2\theta \leq 45^\circ$
temperature	21°C	-100(2)°C
take-off angle	1.0°	1.0°
radiation used	Mo $K\alpha_1$ (0.70926Å)	Mo $K\alpha_1$ (0.70926Å)
lattice constants	$\underline{a} = 8.370(2)\text{Å}$ $\underline{b} = 6.877(1)\text{Å}$ $\underline{c} = 9.244(2)\text{Å}$	$\underline{a} = 11.307(2)\text{Å}$ $\underline{b} = 25.490(5)\text{Å}$ $\underline{c} = 8.316(2)\text{Å}$ $\underline{\beta} = 96.90(1)^\circ$
unit cell volume	$V = 532.07(1)\text{Å}^3$	$V = 2379.42(1)\text{Å}^3$
calculated density	$d_c = 2.08\text{g/cm}^3$	$d_c = 1.79\text{g/cm}^3$ (at 22°C)
measured density	$d_m = 2.03(5)\text{g/cm}^3$	$d_m = 1.74(5)\text{g/cm}^3$ (at 22°C)
Z	4	8
F(000)	336	1320
μ (Mo $K\alpha$)	19.2cm^{-1}	10.0cm^{-1}

...cont'd

Table I : cont'd

STRUCTURE :	I	II
DIFFRACTOMETRY :		
Data Collection :		
radiation used	Mo K α (0.71069Å)	Mo K α (0.71069Å)
temperature	21°C	-100(2)°C
maximum 2 θ angle	60°	45°
take-off angle	3.0°	3.1°
scan width in 2 θ	{ 1.3°+dispersion 1.1°+dispersion	1.3°+dispersion
scan rate in 2 θ	2°/min.	2°/min.
quadrants collected	<u>hkl</u>	<u>hk\bar{l}</u> , <u>$\bar{h}k\bar{l}$</u>
reflections measured	831	1562
reflections observed	566	1331
variables, V	57	222
N/V	9.9	6.0
final R value	0.031	0.031
final R _w value	0.039	0.041

2.3. Diffractometry.

A Picker four-circle diffractometer, automated with the FACS-I system, using niobium-filtered Mo $K\alpha$ radiation ($\lambda=0.71069\text{\AA}$), and a scintillation detector with pulse height analysis, was used for the collection of the unique sets of x-ray diffraction intensity data. The take-off angle was 3.0° for (I) and 3.1° for (II), while the detector with an aperture 5.0 mm high and 4.0 mm wide was positioned 28 cm from the crystal. The computer software used was a 'package' put together by Dr. P.G. Lenhert of Vanderbilt University. The intensity measurements were made at a scan rate of $2^\circ/\text{min.}$ in 2θ with a symmetrical $\theta-2\theta$ scan width of $1.3^\circ + (180/\pi)(2\tan\theta)(\delta\lambda/\lambda)^\circ$; the latter is to account for dispersion of the Mo $K\alpha_1-K\alpha_2$ radiations with increasing 2θ . The background intensity was determined by the normalization of two stationary background counts of 10 sec. measured at both scan limits. Those reflections above 1.8σ were considered as observed reflections; $\sigma = \sqrt{N}$ where N is the scan count plus the total normalized background count.

In both cases, after the crystal was mounted on the diffractometer it was optically aligned to position the crystal precisely at the intercepts of the ϕ and χ circles. To detect a reflection, the reciprocal lattice point had to be brought into contact with the sphere of reflection in the same plane as the x-ray beam, crystal and detector. This was achieved by setting the 2θ value for one reflection with $\chi \approx 0$ or 90° and driving ϕ

until the reflection was located. A second reflection, with $\chi \approx 90^\circ$ away from the first reflection, was then found by setting the 2θ angle and driving χ . The values of 2θ were derived from the preliminary photographic data. Each reflection was carefully centered using an automatic centering routine so as to provide an orientation matrix for the crystal. Both crystals were then deliberately 'misaligned' to a general orientation, in order to eliminate intrinsic multiple reflections^{31,32}, and new orientation matrices were calculated.

For both structures, the accurate cell dimensions were not determined until after the data collection, thus enabling relatively intense, 'high angle' reflections to be selected from the intensity measurements. Unfiltered Mo radiation was used to obtain better counting statistics, and a narrowed detector slit was used so that the Mo $K\alpha_1$ radiation ($\lambda = 0.70926\text{\AA}$) could be more distinctly resolved. The take-off angle was kept small in both cases (1.0°) to give a sharp-parallel incident x-ray beam in order to increase the accuracy of the measurement of the 2θ values. Under these conditions, the cell dimensions were determined by least-squares refinement of the selected reflections whose 2θ values were accurately measured on the diffractometer using the automatic centering routine.

The intensity data for (I) was collected in two 'shells', an inner set of data with $2\theta \leq 40^\circ$, and an outer set of data with $40^\circ < 2\theta \leq 60^\circ$. The outer data was measured in a manner analogous to the inner data, as described above, except that the base scan width

was reduced to 1.1° , since the inner data indicated that it was a little too wide. The two sets of data were initially combined using two scale factors, but this was later considered to be unnecessary as the refined scales differed by less than 1% and the correlation coefficient was very large.

Two standard reflections were measured every 50 reflections for (I) and every 60 reflections for (II), and in both cases retained a constancy within $\pm 2\%$ over the entire data collection. Several reflections for (I) which had a high count rate were remeasured at lower beam intensity and provided no evidence for coincidence losses. No absorption corrections were considered necessary in either case since the absorption coefficient for Mo $K\alpha$ radiation was low for both compounds; in addition, the crystal of (I) was quite small and regular in shape.

It was decided that the data for (II) be collected at low temperature because of the rapid fall-off in the average reflection's intensity with increasing 2θ , as observed in the preliminary photographs taken at room temperature. To measure the reflection intensities at -100°C , an "Air Products and Chemicals" Cryo-Tip refrigerator was adapted for use with the Picker diffractometer. The Cryo-Tip refrigerator is a sub-miniature single-fluid, open cycle Joule-Thomson cooler specifically designed for use in single crystal x-ray diffraction studies. As a technique, the Joule-Thomson cycle is one of the simplest means of achieving cooling because no moving parts are required. The experimental arrangement employed here involved the controlled expansion of nitrogen gas in a chamber mounted on the top of an "Electronics and Alloys"

goniometer head. The crystal selected for the collection of the intensity data was mounted on a copper pin which was supported by a copper rod protruding from the cooling chamber. After the crystal was optically aligned on the diffractometer, the crystal and supporting copper rod was then enclosed by a hollow, cylindrical beryllium shroud which was approximately $3/8$ inch in diameter and 0.003 inch thick. The stainless steel base of the shroud fitted over an o-ring assembly on top of the cooling chamber such that a vacuum tight fit was obtained. The resultant enclosed space around the crystal could then be evacuated via a small, coiled and flexible plastic tube which lead from this assembly to a vacuum pump. The purpose of this evacuated space was two-fold. Firstly, to prevent a build-up of ice on the end of the goniometer head and on the crystal, and secondly, to maintain a more reliably constant and more easily measureable temperature at the crystal. The commercially available compressed nitrogen was passed through a molecular seive, to remove any water present, prior to being regulated and carried to the cooling chamber via a small, coiled and flexible stainless steel tube. The expanded gas was carried away from the cooling chamber via a second small, coiled and flexible plastic tube to a back-pressure regulator. The temperature of the crystal was monitored with an iron-constantan thermocouple mounted at the base of the copper pin.

Prior to the collection of the intensity data for (II), a low temperature precession photograph of the $h0l$ zone was taken using Cu $K\alpha$ radiation ($\lambda = 1.5418\text{\AA}$) to ensure that the crystal did not undergo a phase change upon lowering of the temperature.

In addition to this precaution, the possibility that the intensity of some reflections might be affected by Cu powder lines arising from the copper pin had to be checked. To do this, the measured and calculated structure factors for (II) were sorted according to the 2θ value such that they could be readily compared to the 2θ values of the Cu powder lines. Those reflections which coincided with, or were close to, any of the Cu powder lines did not appear to be in poorer agreement than the other reflections.

CHAPTER 3

ANALYSIS OF THE DIFFRACTION DATA

A description of the computations and computer programs utilized in the analysis of the diffraction data is provided in Appendix A. The raw intensity data had Lorentz and polarization factors applied and was converted into observed structure factors, F_o . Both the observed and calculated structure factors for compounds (I) and (II) are presented in Appendix B.

3.1. Structure Determination For $\text{NH}_4[\text{VO}(\text{O}_2)_2(\text{NH}_3)]$.

An examination of the unsharpened three-dimensional Patterson function based on the observed data indicated that the vanadium atom occupied a special position of the type $x \frac{1}{4} z$. This vanadium atom position ($x/a = 0.23$, $y/b = \frac{1}{4}$, $z/c = 0.225$) was used to initiate phasing of the data such that the conventional unweighted agreement factor (R value†) for the structure factors was 0.353. A three-dimensional electron density map was then computed from the partially phased data, and the remaining nonhydrogen atom positions were deduced from the peaks in this map on the basis of their chemical reasonableness. A full-matrix least-squares refinement on these atomic positional and isotropic temperature parameters subsequently brought the R value down to 0.079. At this point in the structure determination, a series of electron density difference maps, each followed by a full-matrix least-

† The R value is defined as $\Sigma(|F_o| - |F_c|) / \Sigma |F_o|$.

squares refinement, revealed the hydrogen atoms and anisotropic thermal motion of the nonhydrogen atoms in the anion. With these features added to the model, full-matrix least-squares refinement improved the agreement to $R = 0.035$. An examination of the electron density difference map and a close analysis of the variation of agreement between $|F_o|$ and $|F_c|$ as a function of $|F_o|$, and of $(\sin\theta)/\lambda$, was then carried out. From this it was suggested that some of the atomic scattering curves might require adjustment to compensate for atomic charge. In response, curves corresponding to $V^{3\oplus}$ (for the vanadium atom), O^{\ominus} (for the peroxy oxygens), and N^{\oplus} (for the ammonium nitrogen) were introduced into the model, and least-squares refinement gave a final unweighted R value of 0.031 and a weighted R_w value† of 0.039.

The data were given unit weights in the refinement until an R value of 0.035 had been achieved. Refinement to convergence was then carried out with $\sigma = \sqrt{AB/F}$ for $F \leq 12.5$, and $\sigma = \sqrt{AF/B}$ for $F > 12.5$, where $w = 1/\sigma^2$, $A = 0.21$ and $B = 12.5$. This weighting scheme was determined empirically by adjusting the value of A until the error of fit, $[\sum w(|F_o| - |F_c|)^2 / (NO - NV)]^{\frac{1}{2}}$, where (NO - NV) is the number of observations minus the number of variables, was 1.00, i.e. to obtain correct absolute weights. The value of B was adjusted to obtain correct relative weights. The unobserved reflections, which have a magnitude of $\sigma/2$ and appear with negative values of F_o in Appendix B, were excluded from the refinement.

† The R_w value is defined as $[\sum w(|F_o| - |F_c|)^2 / \sum w F_o^2]^{\frac{1}{2}}$.

A final electron density difference synthesis showed, as its major feature, a peak of height $0.48 \text{ e}/\text{\AA}^3$ at the position $(x/a = 0.32, y/b = \frac{1}{4}, z/c = 0.22)$. This position is almost centrally located between the vanadium and vanadyl oxygen atoms. Since this residual electron density is in accordance with previously observed electron density distributions³³, it is felt that this peak can be attributed to increased electron density arising from the V=O double bond.

The scattering factors for the nonhydrogen atoms, including anomalous scattering for the vanadium atom, were taken from reference 34, while the scattering factors for the hydrogen atoms were taken from a table of Stewart et. al.³⁵. The N^{\oplus} scattering curve was obtained by averaging the scattering curves for C and $\text{O}^{2\oplus}$, and differed from the nitrogen scattering curve by no more than 0.05 electron above $(\sin\theta)/\lambda = 0.35$. This latter point is important since 'high angle' x-ray diffraction is the result of the x-rays interacting with the 'core electrons' which should not be significantly affected by the valence shell electrons, and thus atomic charge.

The positional and thermal parameters for (I), obtained in the final least-squares refinement cycle, are listed in Table II, while the interatomic distances and angles are tabulated in Table III. Errors in the interatomic distances and angles were calculated from the inverse matrix and include correlation between atomic parameters and the errors in the cell dimensions.

Figure 1 shows the coordination geometry within the $[\text{VO}(\text{O}_2)_2(\text{NH}_3)]^{\ominus}$ anion; the nonhydrogen atoms are represented as 50% probability thermal ellipsoids. The basal atoms of the anion

are distorted out of a plane, i.e. the atoms O(2), O(3), N(1) and the mirror-related oxygen atoms of the second peroxy group describe an approximate plane. The equation of this plane and the deviations of the atoms from it are given in Table IV. The packing of the molecules in the unit cell is presented as a stereoscopic diagram in Figure 2; the atoms are again represented as 50% probability thermal ellipsoids.

Analysis of the thermal motion³⁶ of the atoms in the anion indicate that their motion can well be approximated to that of a rigid-body, when the appropriate constraints are maintained to preserve the mirror symmetry. This motion has a significant effect on the bond lengths, and the corrected values are given in Table III and are used throughout the discussion. Table V indicates the eigenvectors of T and ω , along with their direction cosines, obtained from the rigid-body analysis. The rms ΔU_i was $0.003(4)\text{\AA}^2$, indicating a good fit between the 'observed' thermal motion and that based on a rigid-body model.

Table II : Final Positional And Thermal Parameters For
NH₄[VO(O₂)₂(NH₃)] .

Atom	x/a	y/b	z/c	U, Å ²
V	0.2304(1) ^a	$\frac{1}{4}$	0.2248(1)	b
O(1)	0.4061(3)	$\frac{1}{4}$	0.1569(4)	b
O(2)	0.2340(3)	0.4405(4)	0.3692(3)	b
O(3)	0.1662(3)	0.5105(3)	0.2329(3)	b
N(1)	0.1026(5)	$\frac{1}{4}$	0.0295(4)	b
N(2)	0.0685(5)	$\frac{1}{4}$	0.6269(5)	0.030(1)
H(1)	0.059(10)	$\frac{1}{4}$	0.539(10)	0.100(30)
H(2)	0.152(11)	$\frac{1}{4}$	0.650(10)	0.099(30)
H(3)	0.038(4)	0.162(6)	0.644(4)	0.039(11)
H(4)	0.006(9)	$\frac{1}{4}$	0.050(8)	0.080(25)
H(5)	0.124(5)	0.155(6)	-0.017(4)	0.044(11)

Atom	U ₁₁ ^b	U ₂₂	U ₃₃	U ₁₂	U ₁₃	U ₂₃
	0.0202(4)	0.0266(2)	0.0203(4)	0.0	0.0039(4)	0.0
1)	0.0248(14)	0.0484(19)	0.0350(17)	0.0	0.0082(12)	0.0
2)	0.0426(14)	0.0670(19)	0.0389(13)	-0.0143(15)	0.0071(12)	-0.0277(13)
3)	0.0457(14)	0.0273(10)	0.0541(13)	-0.0035(9)	0.0168(12)	-0.0077(13)
4)	0.0326(21)	0.0385(24)	0.0264(22)	0.0	-0.0008(16)	0.0

^a Estimated standard deviations of the least significant figures are given in parentheses here and in subsequent tables.

^b The form of the anisotropic thermal ellipsoid is

$$\exp[-2\pi^2(U_{11}h^2a^{*2} + U_{22}k^2b^{*2} + U_{33}l^2c^{*2} + 2U_{12}hka^*b^* + 2U_{13}hla^*c^* + 2U_{23}klb^*c^*)]$$

Table III : Interatomic Distances (Å) And Angles (Deg.) For
NH₄[VO(O₂)₂(NH₃)] .

(a) Bonded Contacts:

V-O(1)	1.599(3) [1.606] ^a	N(1)-H(4)	0.81(4)
V-O(2)	1.871(3) [1.882]	N(1)-H(5)	0.83(8)
V-O(3)	1.872(3) [1.883]	N(2)-H(1)	0.82(9)
V-N(1)	2.098(4) [2.110]	N(2)-H(2)	0.73(10)
O(2)-O(3)	1.463(4) [1.472]	N(2)-H(3)	0.67(4)

(b) Interionic Contacts (Between Nonhydrogen Atoms)

Shorter Than 3.0 Å :

V...O(1)	($-\frac{1}{2}+x, \frac{1}{2}-y, \frac{1}{2}-z$) ^b	2.926(3)
O(1)...N(2)	($\frac{1}{2}+x, \frac{1}{2}-y, \frac{1}{2}-z$)	2.955(6) ^c
O(2)...N(1)	($\frac{1}{2}-x, 1-y, \frac{1}{2}+z$)	2.932(4) ^c
O(3)...O(1)	($-\frac{1}{2}+x, \frac{1}{2}-y, \frac{1}{2}-z$)	2.997(3)
O(3)...N(2)	($-x, \frac{1}{2}+y, 1-z$)	2.872(4) ^c
O(3)...N(1)	($\frac{1}{2}-x, 1-y, -\frac{1}{2}+z$)	2.933(4) ^c

(c) Interionic Contacts (Involving Hydrogen Atoms)

Shorter Than 2.5 Å :

O(1)...H(1)	($\frac{1}{2}+x, \frac{1}{2}-y, \frac{1}{2}-z$)	2.22(9) ^c
O(3)...H(2)	($\frac{1}{2}-x, 1-y, -\frac{1}{2}+z$)	2.37(7) ^c
O(3)...H(3)	($-x, \frac{1}{2}+y, 1-z$)	2.31(4) ^c

...cont'd

Table III : cont'd

(d) Bond Angles:

O(1)-V-O(2)	105.4(1)	V-N(1)-H(4)	108(5)
O(1)-V-O(3)	106.3(1)	V-N(1)-H(5)	111(3)
O(1)-V-N(1)	97.5(2)	H(4)-N(1)-H(5)	110(4)
O(2)-V-O(3)	46.0(1)	H(1)-N(2)-H(2)	113(8)
O(2)-V-N(1)	128.5(1)	H(1)-N(2)-H(3)	101(4)
O(2)-V-O(2) ^a	88.9(1)	H(2)-N(2)-H(3)	107(4)
O(3)-V-N(1)	83.6(1)		
O(3)-V-O(3) ^b	146.3(1)		

(e) Interionic Contact Angles:

O(1)-V.....O(1)	$(-\frac{1}{2}+x, \frac{1}{2}-y, \frac{1}{2}-z)$	178.8(4)
V-O(1)...V	$(\frac{1}{2}+x, \frac{1}{2}-y, \frac{1}{2}-z)$	135.0(2)
N(2)-H(1)...O(1)	$(-\frac{1}{2}+x, \frac{1}{2}-y, \frac{1}{2}-z)$	150(8) ^c
N(2)-H(2)...O(3)	$(\frac{1}{2}-x, 1-y, \frac{1}{2}+z)$	130(3) ^c
N(2)-H(3)...O(3)	$(-x, -\frac{1}{2}+y, 1-z)$	140(5) ^c
N(1)-H(4)...O(2)	$(-\frac{1}{2}+x, \frac{1}{2}-y, \frac{1}{2}-z)$	151(1) ^c

^a Corrected for rigid-body motion.

^b Symmetry transformation applies to the coordinates of the last atom.

^c Possible hydrogen bonds.

Table IV : Mean Plane For $\text{NH}_4[\text{VO}(\text{O}_2)_2(\text{NH}_3)]$.

The mean plane is given as $Ax + By + Cz + D = 0^a$ for the distorted basal plane^b (excluding the vanadium atom) :

$$(0.9420)x + (0.0000)y + (-0.3355)z + (-0.6587) = 0$$

Atom	Deviation From The Plane, Å
V	0.461(1)
O(2)	0.042(3)
O(3)	-0.071(3)
N(1)	0.059(4)

^a The normal equation of a plane, expressed in ångströms, refers to the set of axes x, y, z (corresponding to the lattice constants a, b, and c, respectively).

^b This plane provides only an approximate description of the structure; there are highly significant departures from planarity.

Table V : T (Å²) And ω (Deg.²) Eigenvectors And Direction Cosines
From The Rigid-Body Analysis For NH₄[VO(O₂)₂(NH₃)].

Eigenvectors

of T	Direction Cosines*		
0.0290	0.0000	1.0000	0.0000
0.0264	0.6651	0.0000	0.7467
0.0184	0.7467	0.0000	-0.6651

Eigenvectors

of ω	Direction Cosines*		
39.8	0.8007	0.0000	-0.5991
15.2	0.5991	0.0000	0.8007
13.1	0.0000	-1.0000	0.0000

*Relative to orthogonal axes parallel to a, b, and c.

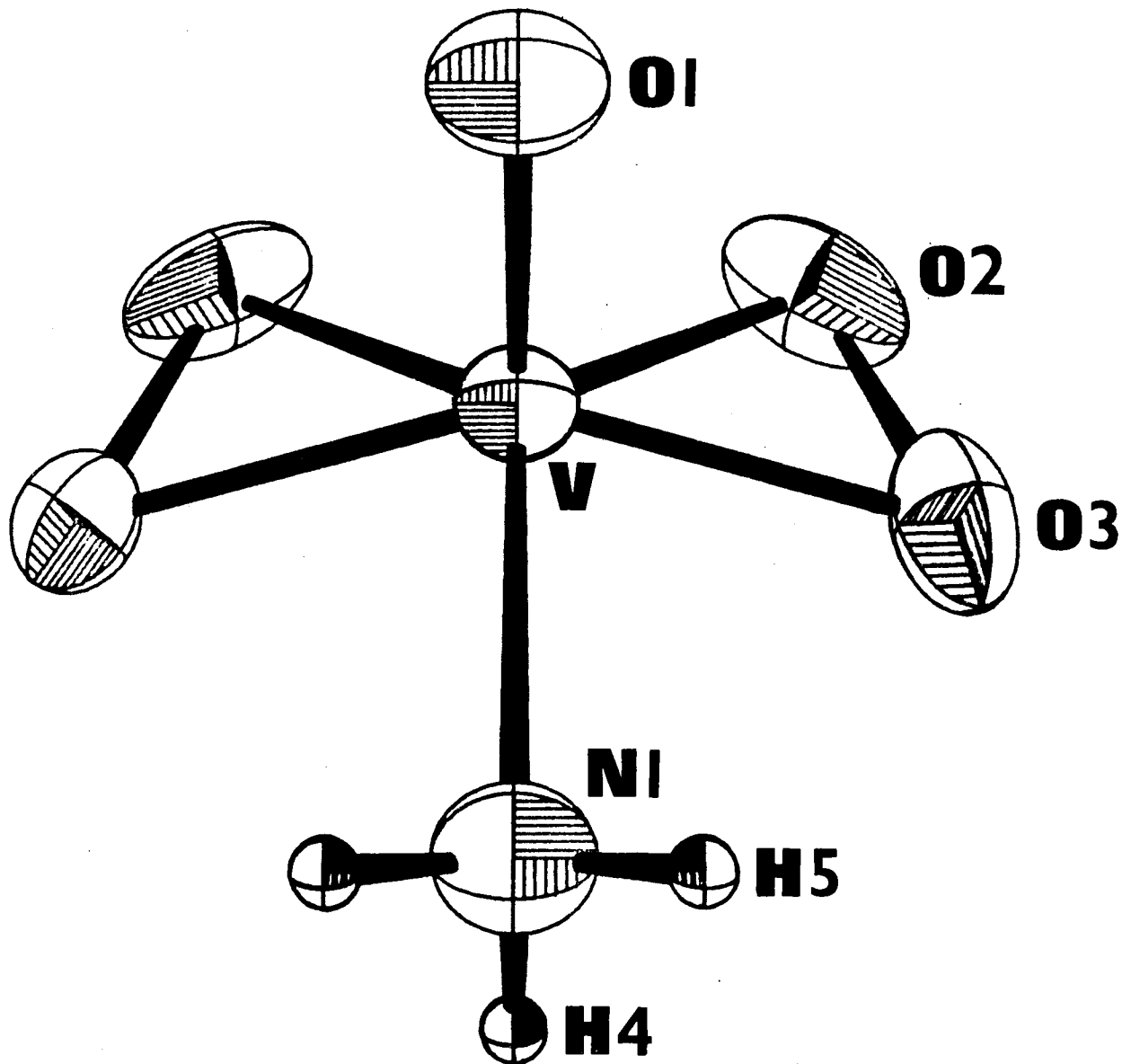


Figure 1 : The $[\text{VO}(\text{O}_2)_2(\text{NH}_3)]^\ominus$ Anion.

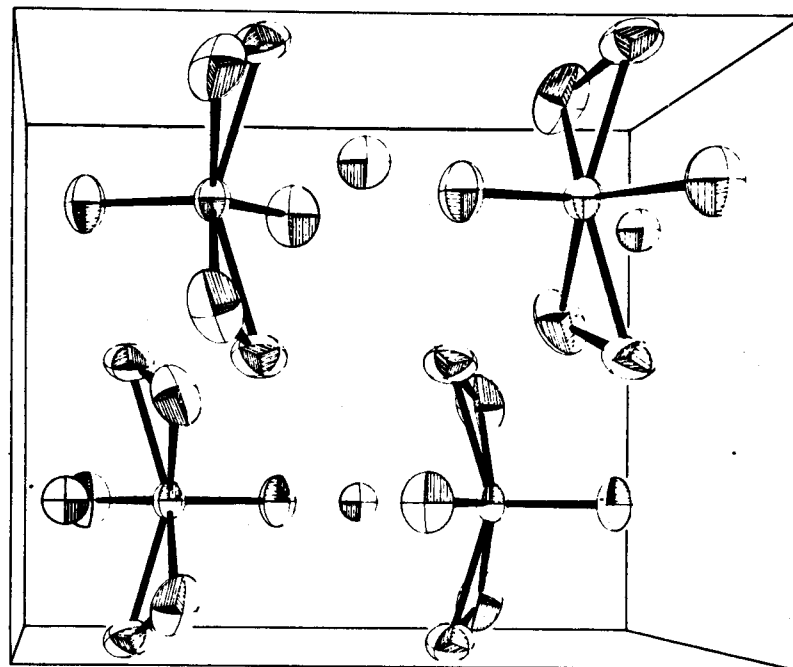
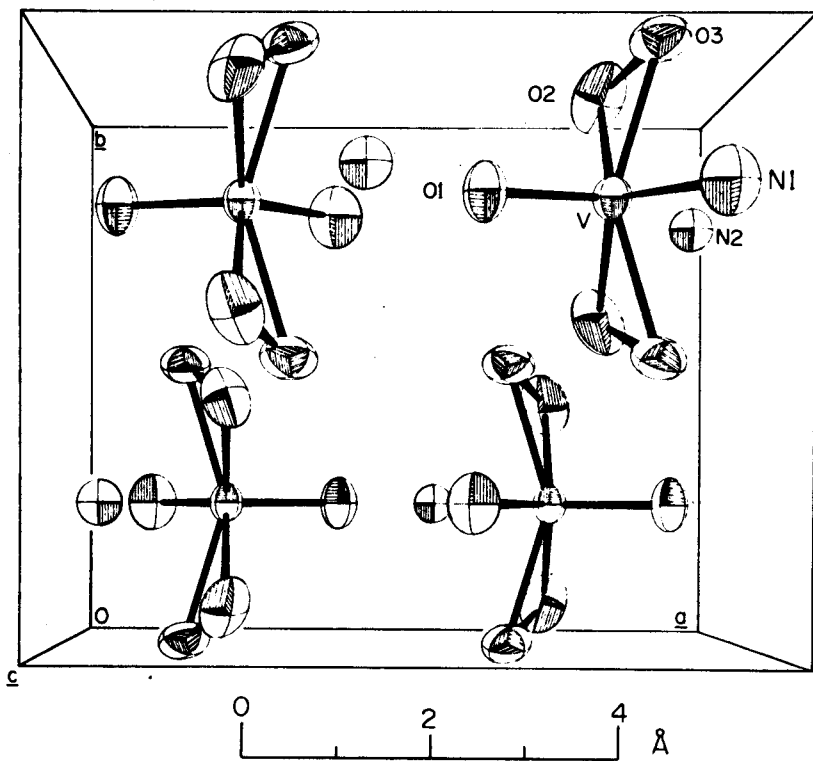
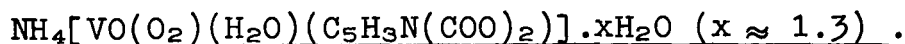


Figure 2 : Stereoscopic Crystal Packing Diagram For $\text{NH}_4[\text{VO}(\text{O}_2)_2(\text{NH}_3)]$.

3.2. Structure Determination For



The symbolic addition procedure (SAP)^{37,38} was used to initiate the solution of the structure in space group C_2/c . After determination of the E-values, the reflections 0 12 0 ($E = +4.71$) and 6 0 6 ($E = -2.67$) were assigned phases on the basis of Harker-Kasper inequalities³⁹, while the reflections 3 5 2 ($E = +3.39$) and 1 23 3 ($E = -3.32$) were chosen as origin determining reflections and arbitrarily assigned phases. The application of the SAP programs to the data with these origin determining reflections enabled all signs to be deduced in terms of one variable. Of the two possible F_o , fourier maps using those reflections with $E \geq 2.5$, one gave reasonable positions for the vanadium atom and the majority of the remaining nonhydrogen atoms. Refinement of the coordinates and isotropic temperature factors for those atoms by full-matrix least-squares techniques gave an R value of 0.32 . A second electron density map, based on the observed data below $(\sin\theta)/\lambda \leq 0.40$, revealed the remaining nonhydrogen atoms, and further refinement followed by electron density difference syntheses located most of the hydrogen atoms and indicated the presence of anisotropic thermal motion for all nonhydrogen atoms. Refinement up until this point was carried out using only that data with $(\sin\theta)/\lambda \leq 0.40$, and the agreement had dropped to $R = 0.039$. A close examination of electron density difference maps indicated that the water molecule on the two-fold position had only partial occupancy (see below) and that some of the atomic scattering curves

might require adjustment to compensate for atomic charge, as was the case for (I). The occupancy for atom O(10) was allowed to vary and curves corresponding to $V^{3\oplus}$ (for the vanadium atom), O^{\ominus} (for the peroxy and coordinated carboxylate oxygen atoms), and N^{\oplus} (for the ammonium nitrogen atoms) were introduced to give an R value of 0.033. The remaining hydrogen atom positions around atom N(3) were calculated on the basis of sensible hydrogen bonding, given appropriate occupancies, and allowed to refine with fixed isotropic temperature factors and on all of the data to give a final unweighted R value of 0.031 and a weighted R_w value of 0.041.

Since this model involved two features which needed careful justification, viz. partial occupancy of a water molecule and disorder of a half multiplicity ammonium ion, it was considered prudent to examine the evidence fully. On the basis of residual electron density in the difference map, it was not clear whether there was a water molecule on the two-fold position and an ammonium ion on the centre of symmetry, or vice versa. It was decided that the former resulted in the more satisfactory model for the following reasons. Firstly, disorder on a centre of symmetry is more chemically reasonable for an ammonium ion than it is for a water molecule, although phase changes at low temperature commonly remove this type of feature^{40a}. Secondly, two peaks which could correspond to hydrogen atoms were located near the two-fold axis position whereas numerous appropriate peaks were 'observed' about the centre of symmetry position. Thirdly, the number of possible hydrogen bonds involving the two-fold axis position are fewer than the number of

possible hydrogen bonds involving the centre of symmetry position, as based on the contact distances and angles. This could explain the non-stoichiometry of the water of crystallization. Finally, since this model gave the better agreement, i.e. $R = 0.031$ as opposed to 0.033 , then on the basis of Hamilton's criterion^{40b} it is the better model.

The data was initially given unit weights, but refinement to convergence was carried out with $\sigma = \sqrt{AB/F}$ for $F \leq 10.0$ and $\sigma = \sqrt{AF/B}$ for $F > 10.0$, where $w = 1/\sigma^2$, $A = 0.34$, and $B = 10.0$. The value of A was again adjusted such that the error of fit, $[\sum w(|F_o| - |F_c|)^2 / (NO - NV)]^{1/2}$, was 1.00. All scattering factors used were the same as those used for (I). The unobserved reflections were excluded from the refinement. It was observed that the $I_{0,0,0}$ value for the $2\ 0\ -2$ reflection was underestimated by approximately 40%. Since the intensity of this reflection was exceedingly large, this may have been due to coincidence losses and/or extinction. However, due to the large coefficient which this reflection contributed to both the fourier electron density and difference syntheses, it was decided that it be arbitrarily increased to bring it into good agreement with $F_{0,0,0}$. The effect of doing this would be to very slightly bias the refinement, but enable less biased difference maps to be obtained. In retrospect, however, a possibly better alternative would have been to remove the reflection from the data altogether, since this would give essentially the same difference maps while leaving the refinement unaffected.

A final electron density difference synthesis showed, as its major positive feature, a pair of peaks of height 0.40 and 0.36e/Å³, positioned nearly linearly around the vanadium atom. Their respective distances from the vanadium were 1.20 and 1.25 Å, and the vector defined by the two peaks made an angle of approximately 12° with the O(1)-O(4) vector. These peaks are attributed to uncorrected anisotropic thermal motion of the vanadium atom. The largest negative feature of the final difference map was a trough of depth -0.25 e/Å³ located at the centre of the pyridine ring. This latter feature is most likely due to inaccuracies in the model resulting from the inability to accurately define the shape of the atoms, i.e. describing the atoms in the pyridine ring as 'spheres' resulted in an excess of electron density at the centre of the ring.

The final positional and thermal parameters for (II), obtained in the final least-squares refinement cycle, are listed in Table VI, while the interatomic distances and angles are given in Table VII. Errors in the interatomic distances and angles were calculated from the inverse matrix and include correlation between atomic parameters and errors in the cell dimensions.

Figure 3 shows the coordination geometry within the [VO(O₂)(H₂O)(C₅H₃N(COO)₂)][⊖] anion with the nonhydrogen atoms represented as 50% probability thermal ellipsoids. The equations of the various planes within the anion along with the deviations of the atoms comprising those planes are given in Table VIII. Table IX gives the angles between the planes. Figure 4 is a

projection down the c-axis of the unit cell with the hydrogen bonding shown as dashed lines.

Analysis of the thermal motion³⁶ of the atoms in the anion, excluding O(4), O(6), and O(8), which are bound to only one other atom within the anion, indicates that their motion can best be described in terms of a rigid-body. This motion, however, does not have a significant effect on the bond lengths since the corrected values were in all cases within one standard deviation of the uncorrected values. Table X indicates the eigenvectors of T and ω , and their direction cosines; the rms ΔU_1 , was 0.002(2) Å² which is interpreted as a very good fit of the rigid-body model to the thermal parameters.

Table VI : Final Positional And Thermal Parameters For
NH₄[VO(O₂)(H₂O)(C₅H₃N(COO)₂)]·xH₂O (x ≈ 1.3).

Atom	x/a	y/b	z/c	U, Å ²
V	0.2230(1)	0.0763(1)	0.1915(1)	*
O(1)	0.1433(2)	0.0704(1)	0.3339(3)	*
O(2)	0.3036(2)	0.0121(1)	0.1985(3)	*
O(3)	0.1974(2)	0.0122(1)	0.0839(3)	*
O(4)	0.3286(2)	0.0963(1)	-0.0072(3)	*
O(5)	0.3759(2)	0.0980(1)	0.3345(3)	*
O(6)	0.4827(2)	0.1626(1)	0.4616(3)	*
O(7)	0.0842(2)	0.0989(1)	0.0213(3)	*
O(8)	-0.0456(2)	0.1626(1)	-0.0597(3)	*
O(9)	0.2598(2)	0.3959(1)	0.3244(3)	*
O(10) ^b	0	0.4209(2)	$\frac{1}{4}$	*
N(1)	0.2173(2)	0.1581(1)	0.2030(3)	*
N(2) ^c	$\frac{1}{2}$	0.4671(2)	$\frac{1}{4}$	*
N(3) ^c	0	$\frac{1}{2}$	0	*
C(1)	0.3953(3)	0.1461(1)	0.3731(4)	*
C(2)	0.3027(3)	0.1833(1)	0.2960(4)	*
C(3)	0.3002(3)	0.2373(1)	0.3109(4)	*
C(4)	0.2054(3)	0.2641(1)	0.2264(4)	*
C(5)	0.1181(3)	0.2372(1)	0.1293(4)	*
C(6)	0.1275(3)	0.1834(1)	0.1200(4)	*
C(7)	0.0460(3)	0.1465(1)	0.0180(4)	*
H(1)	0.394(4)	0.114(2)	0.000(5)	0.044
H(2)	0.291(4)	0.100(2)	-0.092(5)	0.044
H(3)	0.363(3)	0.255(2)	0.381(4)	0.038
H(4)	0.199(3)	0.301(2)	0.239(4)	0.044
H(5)	0.052(3)	0.254(2)	0.068(4)	0.038
H(6)	0.327(4)	0.380(2)	0.355(4)	0.038
H(7)	0.264(4)	0.417(2)	0.368(5)	0.038
H(8)	0.051(3)	-0.018(2)	0.221(5)	0.038
H(9)	0.479(3)	0.451(2)	0.168(4)	0.038
H(10) ^d	0.051(3)	0.404(3)	0.289(7)	0.038
H(11) ^c	0.010(13)	0.479(5)	0.069(12)	0.038
H(12) ^c	-0.047(8)	0.526(5)	-0.002(16)	0.038
H(13) ^c	0.038(7)	0.524(4)	0.052(9)	0.038
H(14) ^c	0.044(10)	0.498(6)	-0.071(18)	0.038

...cont'd

Table VI : cont'd

Atom	U ₁₁ ^a	U ₂₂	U ₃₃	U ₁₂	U ₁₃	U ₂₃
V	0.0202 (3)	0.0103 (3)	0.0222 (3)	-0.0008 (2)	-0.0022 (2)	-0.0008 (2)
O (1)	0.0270 (11)	0.0186 (11)	0.0241 (11)	0.0027 (9)	-0.0025 (9)	-0.0010 (8)
O (2)	0.0306 (12)	0.0141 (11)	0.0386 (12)	0.0034 (9)	0.0040 (10)	0.0003 (10)
O (3)	0.0364 (13)	0.0168 (11)	0.0333 (12)	-0.0056 (9)	0.0015 (10)	-0.0082 (9)
O (4)	0.0250 (12)	0.0314 (13)	0.0258 (12)	-0.0119 (10)	-0.0049 (9)	0.0029 (10)
O (5)	0.0227 (11)	0.0122 (12)	0.0302 (11)	0.0034 (8)	-0.0065 (9)	-0.0010 (9)
O (6)	0.0211 (11)	0.0219 (12)	0.0431 (13)	0.0029 (10)	-0.0182 (10)	-0.0062 (10)
O (7)	0.0222 (10)	0.0162 (12)	0.0255 (11)	-0.0043 (9)	-0.0051 (8)	-0.0017 (8)
O (8)	0.0268 (12)	0.0265 (13)	0.0466 (14)	-0.0010 (10)	-0.0211 (11)	0.0067 (11)
O (9)	0.0339 (13)	0.0247 (14)	0.0300 (13)	0.0060 (11)	-0.0092 (10)	-0.0066 (10)
O (10)	0.0235 (33)	0.0290 (35)	0.0273 (32)	0	0.0029 (22)	0
N (1)	0.0185 (13)	0.0145 (13)	0.0242 (13)	0.0006 (11)	-0.0074 (10)	-0.0012 (10)
N (2)	0.0238 (21)	0.0191 (22)	0.0315 (23)	0	-0.0062 (18)	0
N (3)	0.0458 (35)	0.0285 (27)	0.0299 (29)	0.0101 (25)	0.0135 (23)	0.0055 (23)
C (1)	0.0235 (17)	0.0202 (18)	0.0244 (16)	0.0025 (13)	-0.0035 (14)	-0.0003 (13)
C (2)	0.0204 (15)	0.0165 (17)	0.0272 (16)	-0.0008 (13)	-0.0060 (13)	-0.0004 (12)
C (3)	0.0261 (17)	0.0185 (19)	0.0383 (19)	-0.0023 (14)	-0.0099 (15)	-0.0051 (14)
C (4)	0.0337 (19)	0.0122 (18)	0.0497 (21)	0.0031 (14)	-0.0080 (16)	-0.0023 (15)
C (5)	0.0264 (17)	0.0192 (18)	0.0386 (19)	0.0056 (14)	-0.0092 (15)	0.0024 (14)
C (6)	0.0179 (15)	0.0176 (16)	0.0266 (17)	0.0004 (12)	-0.0045 (13)	0.0013 (13)
C (7)	0.0237 (17)	0.0210 (18)	0.0234 (16)	-0.0035 (14)	-0.0036 (14)	0.0025 (13)

^a Anisotropic thermal parameters. The form of the anisotropic thermal ellipsoid is:

$$\exp[-2\pi^2(U_{11}h^2a^{*2} + U_{22}k^2b^{*2} + U_{33}l^2c^{*2} + 2U_{12}hka^{*}b^{*} + 2U_{13}hla^{*}c^{*} + 2U_{23}klb^{*}c^{*})]$$

^b Occupancy 0.311(8) .

^c Multiplicity $\frac{1}{2}$.

^d Occupancy 0.622 .

Table VII : Interatomic Distances (Å) And Angles (Deg.) For
NH₄[VO(O₂)(H₂O)(C₅H₃N(COO)₂)]·xH₂O (x ≈ 1.3) .

(a) Bond Distances:

V-O(1)	1.579(2)	O(4)-H(1)	0.78(4)
V-O(2)	1.870(2)	O(4)-H(2)	0.87(4)
V-O(3)	1.872(2)		
V-O(4)	2.211(2)	C(3)-H(3)	0.97(4)
V-O(5)	2.053(2)	C(4)-H(4)	0.96(4)
V-O(7)	2.064(2)	C(5)-H(5)	0.95(4)
V-N(1)	2.088(2)		
O(2)-O(3)	1.441(3)	O(9)-H(6)	0.65(4)
N(1)-C(2)	1.327(4)	O(9)-H(7)	0.87(4)
N(1)-C(6)	1.325(4)		
C(1)-O(5)	1.280(4)	N(2)-H(8)	0.76(4)
C(1)-O(6)	1.233(4)	N(2)-H(9)	0.81(4)
C(1)-C(2)	1.498(4)		
C(2)-C(3)	1.384(5)	O(10)-H(10)	0.76(7)
C(3)-C(4)	1.388(5)		
C(4)-C(5)	1.380(5)	N(3)-H(11)	0.78(12)
C(5)-C(6)	1.378(5)	N(3)-H(12)	0.85(10)
C(6)-C(7)	1.505(4)	N(3)-H(13)	0.84(8)
C(7)-O(7)	1.288(4)	N(3)-H(14)	0.82(11)
C(7)-O(8)	1.223(4)		

...cont'd

Table VII : cont'd

(b) Bond Angles:

O(1)-V-O(2)	102.3(1)	O(5)-C(1)-O(6)	125.4(3)
O(1)-V-O(3)	101.9(1)	O(5)-C(1)-C(2)	114.1(3)
O(1)-V-O(4)	172.2(1)	O(6)-C(1)-C(2)	120.5(3)
O(1)-V-O(5)	96.2(1)	C(1)-C(2)-N(1)	111.5(3)
O(1)-V-O(7)	94.9(1)	C(1)-C(2)-C(3)	127.7(3)
O(1)-V-N(1)	92.2(1)	N(1)-C(2)-C(3)	120.8(3)
O(2)-V-O(3)	45.3(1)	C(2)-C(3)-C(4)	117.8(3)
O(2)-V-O(4)	85.4(1)	C(2)-C(3)-H(3)	119(2)
O(2)-V-O(5)	81.0(1)	C(4)-C(3)-H(3)	123(2)
O(2)-V-O(7)	126.3(1)	C(3)-C(4)-C(5)	120.4(3)
O(2)-V-N(1)	152.8(1)	C(3)-C(4)-H(4)	120(2)
O(3)-V-O(4)	84.8(1)	C(5)-C(4)-H(4)	120(2)
O(3)-V-O(5)	125.7(1)	C(4)-C(5)-C(6)	118.2(3)
O(3)-V-O(7)	81.6(1)	C(4)-C(5)-H(5)	123(2)
O(3)-V-N(1)	153.0(1)	C(6)-C(5)-H(5)	118(2)
O(4)-V-O(5)	83.0(1)	C(5)-C(6)-C(7)	127.4(3)
O(4)-V-O(7)	81.8(1)	C(5)-C(6)-N(1)	120.9(3)
O(4)-V-N(1)	80.0(1)	N(1)-C(6)-C(7)	111.7(3)
O(5)-V-O(7)	147.2(1)	C(6)-C(7)-O(7)	113.3(3)
O(5)-V-N(1)	74.5(1)	C(6)-C(7)-O(8)	120.7(3)
O(7)-V-N(1)	74.3(1)	O(7)-C(7)-O(8)	126.0(3)
V-O(2)-O(3)	67.3(1)	H(6)-O(9)-H(7)	103(4)
V-O(3)-O(2)	67.4(1)	H(10)-O(10)-H(10) ^a	111(3)
V-O(4)-H(1)	127(3)	H(8)-N(2)-H(8) ^a	121(3)
V-O(4)-H(2)	114(3)	H(8)-N(2)-H(9)	98(3)
H(1)-O(4)-H(2)	111(4)	H(8)-N(2)-H(9) ^a	111(3)
V-O(5)-C(1)	120.7(2)	H(9)-N(2)-H(9) ^a	118(3)
V-O(7)-C(7)	120.2(2)	H(11)-N(3)-H(12)	126(8)
V-N(1)-C(2)	119.0(2)	H(11)-N(3)-H(13)	96(8)
V-N(1)-C(6)	119.2(2)	H(11)-N(3)-H(14)	116(9)
C(2)-N(1)-C(6)	121.8(3)	H(12)-N(3)-H(13)	106(8)
		H(12)-N(3)-H(14)	118(9)
		H(13)-N(3)-H(14)	96(8)

...cont'd

Table VII : cont'd

(c) Interionic/Intermolecular Contacts Less Than 3.2 Å :

O(4)...O(6) ^a	2.714(4)	H(1)...O(6) ^a	1.86(4)
O(4)...O(9) ^b	2.714(4)	H(2)...O(9) ^b	1.95(4)
O(4)...N(3) ^c	3.123(4)	O(4)...H(12) ^e	2.27(8)
C(3)...O(8) ^c	3.202(4)	H(3)...O(8) ^c	2.38(4)
C(5)...O(6) ^c	3.209(4)	H(5)...O(6) ^c	2.40(4)
O(9)...O(8) ^c	2.737(4)	H(6)...O(8) ^c	1.87(4)
O(9)...O(3) ^d	3.083(4)	H(7)...O(3) ^d	2.48(4)
O(9)...O(10) ^f	2.996(4)	O(9)...H(10) ^f	2.35(7)
N(2)...O(3) ^e	2.992(4)	H(8)...O(3) ^e	2.25(4)
N(2)...O(7) ^b	2.882(4)	H(9)...O(7) ^b	2.08(4)
O(10)...N(3) ^f	2.897(4)	O(10)...H(11) ^f	2.13(12)
N(3)...O(5) ^d	3.104(4)	H(13)...O(5) ^d	2.27(8)
N(3)...O(2) ^b	2.938(4)	H(14)...O(2) ^b	2.14(11)

Superscripts indicate the symmetry operation to be applied:

- ^a (-x, +y, $\frac{1}{2}$ -z)
- ^b ($\frac{1}{2}$ -x, $\frac{1}{2}$ -y, -z)
- ^c ($\frac{1}{2}$ +x, $\frac{1}{2}$ -y, $\frac{1}{2}$ +z)
- ^d ($\frac{1}{2}$ -x, $\frac{1}{2}$ +y, $\frac{1}{2}$ -z)
- ^e ($\frac{1}{2}$ +x, $\frac{1}{2}$ +y, +z)
- ^f (+x, +y, +z)
- ^h (+x, -y, $\frac{1}{2}$ +z)

...cont'd

Table VII : cont'd

(d) Interionic/Intermolecular Contact Angles:

V-0(2)...N(3) ^b	118.2(1)	^f 0(9)...0(10)...0(9) ^a	155.5(3)
0(3)-0(2)...N(3) ^b	104.7(3)	^f 0(9)...0(10)...N(3) ^f	102.2(3)
V-0(3)...0(9) ^d	135.3(1)	^f 0(9)...0(10)...N(3) ^b	94.8(3)
V-0(3)...N(2) ^e	101.3(1)	^a 0(9)...0(10)...N(3) ^f	94.8(3)
0(2)-0(3)...0(9) ^d	75.0(3)	^a 0(9)...0(10)...N(3) ^b	102.2(3)
0(2)-0(3)...N(2) ^e	107.6(3)	^f N(3)...0(10)...N(3) ^b	91.7(3)
^d 0(9)...0(3)...N(2) ^e	67.7(3)	^e 0(3)...N(2)...0(3) ^d	134.8(3)
V-0(4)...0(6) ^a	121.7(1)	^d 0(3)...N(2)...0(3) ^b	113.0(3)
V-0(4)...0(9) ^b	125.1(1)	^d 0(3)...N(2)...0(3) ^e	93.3(3)
V-0(4)...N(3) ^e	101.2(1)	^e 0(3)...N(2)...0(7) ^b	93.3(3)
^a 0(6)...0(4)...0(9) ^b	106.4(3)	^e 0(3)...N(2)...0(7) ^e	113.0(3)
^a 0(6)...0(4)...N(3) ^e	90.7(3)	^b 0(7)...N(2)...0(7) ^e	108.7(3)
^b 0(9)...0(4)...N(3) ^e	103.4(3)	^b 0(2)...N(3)...0(4) ^e	125.5(3)
V-0(5)...N(3) ^d	110.2(1)	^b 0(2)...N(3)...0(5) ^d	90.1(3)
C(1)-0(5)...N(3) ^d	127.2(3)	^b 0(2)...N(3)...0(10) ^f	113.3(3)
C(1)-0(6)...C(5) ^e	146.9(3)	^e 0(4)...N(3)...0(5) ^d	67.9(3)
C(1)-0(6)...0(4) ^a	115.5(3)	^e 0(4)...N(3)...0(10) ^f	120.5(3)
^a 0(4)...0(6)...C(5) ^e	96.3(3)	^d 0(5)...N(3)...0(10) ^f	106.3(3)
V-0(7)...N(2) ^b	121.8(1)	0(4)-H(1)...0(6) ^a	168(3)
C(7)-0(7)...N(2) ^b	117.0(3)	0(4)-H(2)...0(9) ^b	163(3)
C(7)-0(8)...C(3) ^e	146.8(3)	C(3)-H(3)...0(8) ^e	143(3)
C(7)-0(8)...0(9) ^e	126.6(3)	C(5)-H(5)...0(6) ^e	143(3)
^e C(3)...0(8)...0(9) ^e	86.2(3)	0(9)-H(6)...0(8) ^e	170(3)
^d 0(3)...0(9)...0(8) ^e	110.0(3)	0(9)-H(7)...0(3) ^d	155(4)
^d 0(3)...0(9)...0(4) ^b	101.5(3)	N(2)-H(8)...0(3) ^e	166(3)
^d 0(3)...0(9)...0(10) ^f	88.2(3)	N(2)-H(9)...0(7) ^b	172(3)
^b 0(4)...0(9)...0(8) ^e	124.7(3)	0(10)-H(10)...0(9) ^f	143(6)
^b 0(4)...0(9)...0(10) ^f	63.0(3)	N(3)-H(11)...0(10) ^f	168(6)
^e 0(8)...0(9)...0(10) ^f	156.2(3)	N(3)-H(12)...0(4) ^e	180(6)
		N(3)-H(13)...0(5) ^d	171(6)
		N(3)-H(14)...0(2) ^b	163(6)

Table VIII : Least-Squares Mean Planes For
 $\text{NH}_4[\text{VO}(\text{O}_2)(\text{H}_2\text{O})(\text{C}_5\text{H}_3\text{N}(\text{COO})_2)] \cdot x\text{H}_2\text{O}$ ($x \approx 1.3$) .

Plane	χ^2	Coefficients*	Atoms Comprising The Plane	Displacements Of The Atoms From The Plane, Å
1	15.8	0.6452	O(2)	0.000(2)
		0.1784	O(3)	0.003(2)
		-0.7429	O(5)	-0.004(2)
		-0.9239	O(7)	-0.005(2)
			N(1)	0.005(2)
2	3.1	0.6138	O(5)	0.002(2)
		0.1090	C(1)	-0.003(3)
		-0.7819	C(2)	0.003(3)
		-0.5142	N(1)	-0.002(2)
3	239.9	0.6335	O(7)	0.015(2)
		0.1741	C(6)	0.024(3)
		-0.7539	C(7)	-0.025(3)
		-0.8808	N(1)	-0.014(2)
4	744.2	-0.7573	V	-0.012(1)
		0.0055	O(1)	0.009(2)
		-0.6530	O(4)	0.007(2)
		2.7734	C(4)	0.002(3)
			N(1)	-0.006(2)
5	13.8	0.6230	N(1)	-0.006(2)
		0.0922	C(2)	0.000(3)
		-0.7767	C(3)	0.005(3)
		-0.4799	C(4)	-0.005(4)
			C(5)	0.000(3)
			C(6)	0.005(3)
6	19.5	0.6062	O(5)	0.003(2)
		0.1045	O(6)	0.004(2)
		-0.7884	C(1)	-0.010(3)
		-0.4535	C(2)	0.003(3)
7	4.8	0.5958	O(7)	0.002(2)
		0.1869	O(8)	0.002(2)
		-0.7811	C(6)	0.001(3)
		-0.8861	C(7)	-0.005(3)

* These are coefficients for the normal equation of a plane in the form $Ax + By + Cz + D = 0$, expressed in ångströms, referring to the set of axes x, y, z ; corresponding to \underline{a} , \underline{b} , and \underline{c}^* , respectively.

Table IX : Angles Between The Least-Squares Mean Planes For
 $\text{NH}_4[\text{VO}(\text{O}_2)(\text{H}_2\text{O})(\text{C}_5\text{H}_3\text{N}(\text{COO})_2)] \cdot x\text{H}_2\text{O}$ ($x \approx 1.3$) .

Planes*	Angle (degrees)	Planes	Angle (degrees)
1-2	4.9	3-4	89.2
1-3	1.0	3-5	4.9
1-4	90.2	3-6	4.7
1-5	5.5	3-7	2.8
1-6	5.5	4-5	88.0
1-7	3.6	4-6	86.8
2-3	4.2	4-7	86.6
2-4	87.3	5-6	1.4
2-5	1.1	5-7	5.7
2-6	1.4	6-7	4.8
2-7	5.7		

* These planes are defined in Table VIII.

Table X : T (\AA^2) And ω (Deg.²) Eigenvectors And Direction Cosines From The Rigid-Body Analysis For $\text{NH}_4[\text{VO}(\text{O}_2)(\text{H}_2\text{O})(\text{C}_5\text{H}_3\text{N}(\text{COO})_2)] \cdot x\text{H}_2\text{O}$ ($x \approx 1.3$) .

Eigenvectors

of T	Direction Cosines*		
0.0279	-0.6891	-0.0738	0.7209
0.0156	-0.7156	0.2260	-0.6610
0.0133	-0.1139	-0.9714	-0.2082

Eigenvectors

of ω	Direction Cosines*		
6.3	-0.9530	-0.2496	-0.1719
4.3	-0.0326	-0.4628	0.8859
2.4	-0.3010	0.8470	0.4381

* Relative to orthogonalized axes parallel to a, b, and c.*

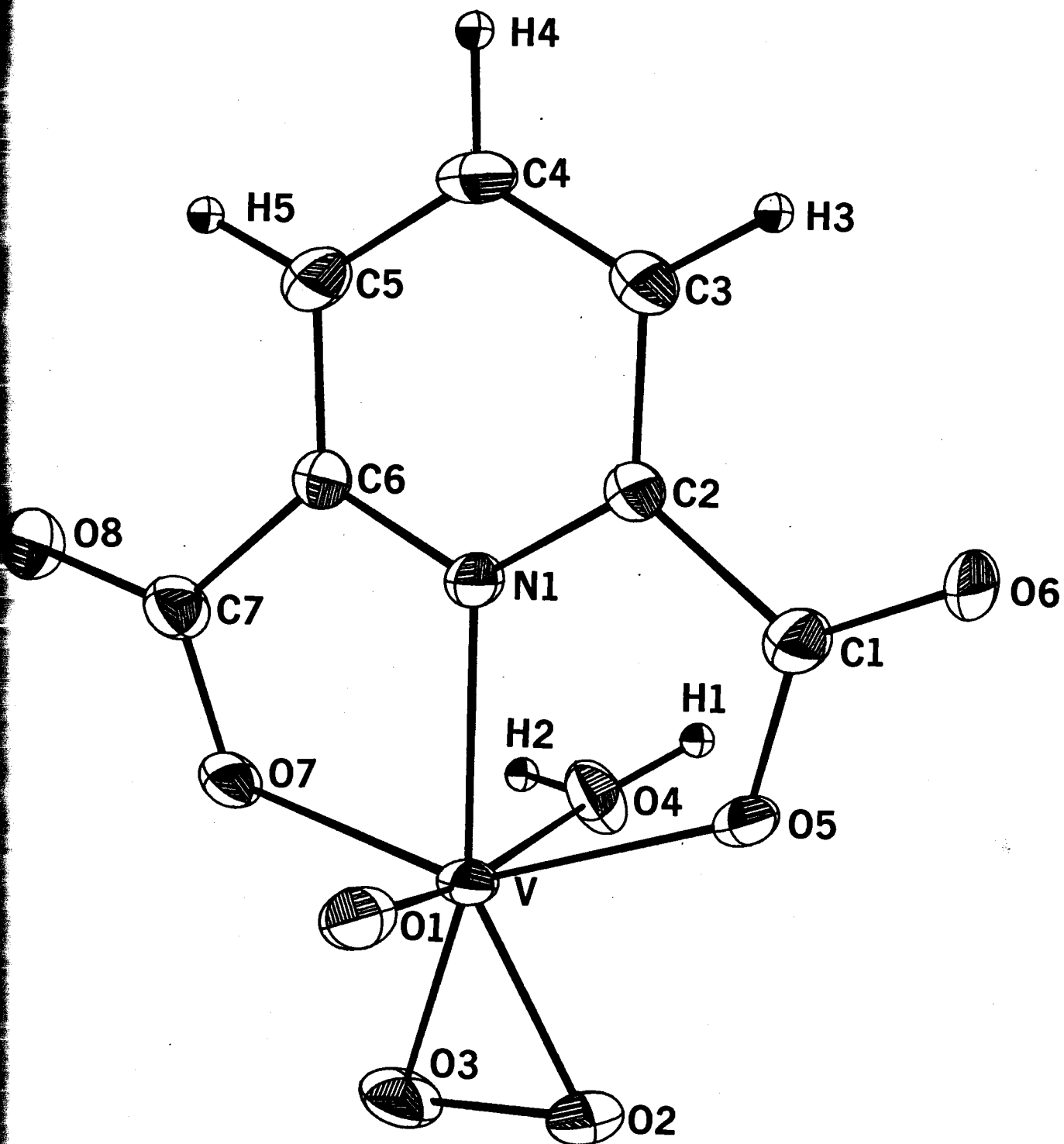


Figure 3 : The $[VO(O_2)(H_2O)(C_5H_3N(COO)_2)]^-$ Anion.

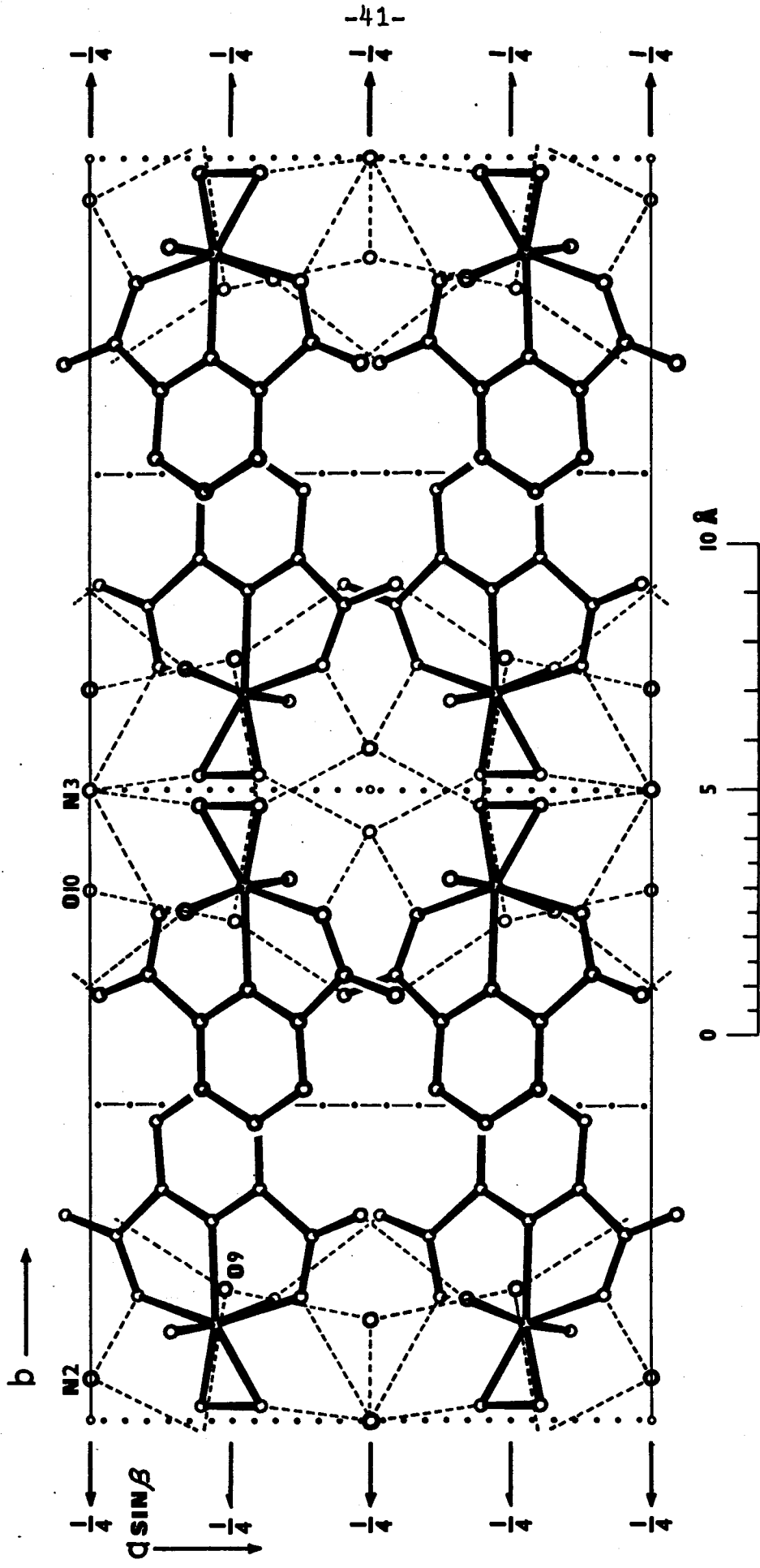


Figure 4 : A Projection Down The c -axis Of The Unit Cell For $\text{NH}_4[\text{VO}(\text{O}_2)(\text{H}_2\text{O})(\text{C}_5\text{H}_3\text{N}(\text{COO})_2)] \cdot x\text{H}_2\text{O}$ ($x \approx 1.3$). The hydrogen bonds are shown as dashed lines.

CHAPTER 4

DISCUSSION OF THE RESULTS

4.1. $\text{NH}_4[\text{VO}(\text{O}_2)_2(\text{NH}_3)]$.

The compound (I) consists of four formula units in the primitive orthorhombic unit cell (see Figure 2). Both the cation and the anion lie on the mirror plane, with half of each ion comprising the asymmetric unit. The vanadium atom is bonded to five oxygen atoms and one nitrogen atom in what can best be described as a pentagonal pyramid, the four oxygen atoms of the two peroxy groups, which are related by the mirror plane, and the nitrogen atom of the NH_3 group forming the base of the distorted pyramid, while the vanadyl oxygen atom occupies the apical position. Thus, the coordination geometries in the $[\text{VO}(\text{O}_2)_2(\text{NH}_3)]^\ominus$ anion and in the oxodiperoxopyridinechromium(VI) complex¹³, $[\text{CrO}(\text{O}_2)_2(\text{C}_5\text{H}_5\text{N})]$, are not significantly different.

The vanadium atom is not coplanar with the 'basal pentagon' but is displaced 0.46 Å toward the vanadyl oxygen O(1). Distortions of this type are commonly found in oxovanadium(V) complexes⁴¹ and can be attributed⁴² to the repulsions which result between the vanadium-oxygen π -bonding and the σ -bonds of the basal plane. In the complex $[\text{CrO}(\text{O}_2)_2(\text{C}_5\text{H}_5\text{N})]$ ¹³, the chromium atom was similarly displaced by 0.51 Å, while in the pentagonal-bipyramidal complexes $[\text{VO}(\text{NO}_3)_3 \cdot \text{CH}_3\text{CN}]$ ⁴³, $(\text{NH}_4)_4[\text{O}(\text{VO}(\text{O}_2)_2)_2]$ ⁵, $[\text{CrO}(\text{O}_2)_2(\text{C}_{10}\text{H}_8\text{N}_2)]$ ¹⁴, and $[\text{CrO}(\text{O}_2)_2(\text{C}_{12}\text{H}_8\text{N}_2)]$ ¹⁵, the metal atoms were observed to be displaced out of the equatorial plane toward

the apical oxide oxygen atom by 0.27, 0.43*, 0.31, and 0.27 Å, respectively. These complexes of V(V) and Cr(VI) suggest that the observed displacements of the metal atoms from the plane are significantly greater in the pentagonal-pyramidal complexes than in the pentagonal-bipyramidal complexes, as might be expected.

The short V-O(1) bond length of 1.606(3) Å is indicative of a vanadium-oxygen double bond. It is slightly longer than V=O bond lengths in some other vanadium(V) compounds, e.g. [VO(NO₃)₃.CH₃CN] ⁴³, 1.55(2)Å; VO(OCH₃)₃ ⁴¹, 1.51(5) and 1.58(4)Å; VOCl₃ ⁴⁴, 1.56(4)Å; but slightly shorter than the V=O bond length of 1.612(10)Å observed for the vanadium(IV) compound VO(C₆H₅-CH₂COO)₂ ⁴⁵. The V-NH₃ distance of 2.110(4)Å is not representative of a strong coordination of the NH₃ group, but it is much stronger than the V-NCCH₃ coordination distance of 2.24(3)Å in the complex [VO(NO₃)₃.CH₃CN] ⁴³.

The O(2)-O(3) bond length of 1.472(4)Å in the peroxo groups is slightly shorter than the 1.49Å accepted^{1,46} for the O₂²⁻ entity but significantly longer than the mean O-O bond lengths of 1.404(16)Å observed in [CrO(O₂)₂(C₅H₅N)] ¹³ and 1.40(2)Å observed in

*The complex (NH₄)₄[O(VO(O₂)₂)₂] is described as pentagonal-bipyramidal, but, in fact, the seventh coordination site is occupied as a close contact; as a result, the displacement distance of 0.43 Å is closer to the displacement observed in (I) than the displacements observed for the truly pentagonal-bipyramidal complexes.

$[\text{CrO}(\text{O}_2)_2(\text{C}_{10}\text{H}_8\text{N}_2)]$ ¹⁴ and $[\text{CrO}(\text{O}_2)_2(\text{C}_{12}\text{H}_8\text{N}_2)]$ ¹⁵. It is also longer, but not significantly, than the mean O-O bond length of 1.44Å observed for $(\text{NH}_4)_4[\text{O}(\text{VO}(\text{O}_2)_2)_2]$ ⁵. This shortening of the peroxy bond has been observed^{1,46} in most transition metal peroxy complexes and is attributed to the mode of coordination of the peroxy group^{1,46,47}, i.e. the symmetrical coordination of the peroxy group and the resultant withdrawal of electron density from the anti-bonding π^*2p_y orbitals on the peroxy group to the empty d_{xy} and $d_{x^2-y^2}$ orbitals on the metal atom. In other words, the more strongly the peroxy group is coordinated to the metal atom, the shorter the O-O bond length. The vibrational spectra of the complexes (I) and $[\text{CrO}(\text{O}_2)_2(\text{C}_5\text{H}_5\text{N})]$ ¹³ both show infrared stretching frequencies for the peroxy group⁴⁷⁻⁴⁹ at 880 cm^{-1} , a somewhat surprising observation considering how significantly different the peroxy bond lengths appear to be in these two complexes.

The V-O(2) and V-O(3) bond lengths of 1.882(3) and 1.883(3)Å, respectively, show that the peroxy group is truly symmetrically π -bonded to the vanadium atom. These bonds are significantly shorter than the mean V-O bond lengths of 2.05(4)Å for the bidentate nitrates and only slightly shorter than the V-ONO₂ bond length of 1.92(2)Å observed for the monodentate nitrate in $[\text{VO}(\text{NO}_3)_3 \cdot \text{CH}_3\text{CN}]$ ⁴³. They are comparable to the mean V-O_{peroxy} bond lengths of 1.87Å in $(\text{NH}_4)_4[\text{O}(\text{VO}(\text{O}_2)_2)_2]$ ⁵ and 1.89Å in $(\text{NH}_4)_3[\text{V}(\text{O}_2)_4]$ ⁵, but slightly longer than the mean Cr-O_{peroxy} bond length of 1.82(4)Å in $[\text{CrO}(\text{O}_2)_2(\text{C}_5\text{H}_5\text{N})]$ ¹³, as one might expect from the O-O bond lengths. This is also consistent with the expectation that V(V) has a larger covalent radius than Cr(VI),

which is further supported by the fact that the V=O and V-N bonds are slightly longer than the corresponding Cr=O and Cr-N bonds.

One of the shortest intermolecular contacts involving nonhydrogen atoms is between the vanadium atom and the vanadyl oxygen atom of a second anion. The V...O(1) distance is 2.926(3)Å, while the O(1)-V...O(1) and V-O(1)...V angles are 178.8(1)° and 135.0(2)°, respectively (see Table III). This distance is shorter than the sum of the van der Waals radii, but still too long to be considered a formal bond, and is most likely a dipolar interaction which results in a more satisfactory environment for the vanadium atom. Such a contact might allow one to consider the environment around the vanadium atom as very weakly tending toward a distorted pentagonal-bipyramid. Indeed the slightly lengthened V=O bond and smaller displacement of the vanadium atom out of the 'basal plane', compared to the chromium analog [CrO(O₂)₂(C₅H₅N)]¹³, may well reflect this long interaction. This is similar, but less extreme, to what was observed for (NH₄)₄[O(VO(O₂)₂)₂]⁵. While the average V=O bond length of 1.61Å is comparable, the observed contact distances were 2.48 and 2.52Å, which are very short, and as already indicated above, is reflected in the displacement of the vanadium atom out of the equatorial plane. Of the remaining intermolecular contacts between nonhydrogen atoms which are less than 3.0Å, the majority appear to be weak hydrogen bonds. The details of these are presented in Table III.

The observed mean N-H bond length of 0.80(10)Å is comparable to the mean N-H bond length of 0.88(4)Å observed in the compound

$\text{Cr}(\text{CO}_2\text{CH}_2\text{NH}_2)_3 \cdot \text{H}_2\text{O}$ ⁵⁰. Considering the distortion in the electron density distribution normally encountered in x-ray studies^{40a} for hydrogen atoms, the observed distances are close to the expected values.

Finally, returning to the coordination geometry of the vanadium atom, an alternative view^{43,51} can be proposed in which the metal atom is formally four-coordinate in a distorted tetrahedral arrangement, each peroxo group bonding with one coordination site, e.g. a vacant sd^3 hybrid, by means of a three-centre bond. Such a proposal is not unreasonable, especially when the bond angles to the midpoints of the peroxo groups are examined: $\text{O}(1)\text{-V}\text{-(O}_2)$, $107.2(1)^\circ$; $\text{O}(1)\text{-V}\text{-N}(1)$, $97.5(1)^\circ$; $\text{N}(1)\text{-V}\text{-(O}_2)$, $106.1(1)^\circ$; $\text{(O}_2)\text{-V}\text{-(O}_2)$, $128.5(1)^\circ$. The largest angle is attributed⁴⁶ to repulsion between the two peroxo groups, and the smallest angle is a 'response' to this repulsion by the less strongly bound NH_3 group. This angle of $128.5(1)^\circ$ is not, however, as large as corresponding angles observed⁴⁶ in the diperoxochromium(VI) complexes.

4.2. $\text{NH}_4[\text{VO}(\text{O}_2)(\text{H}_2\text{O})(\text{C}_5\text{H}_3\text{N}(\text{COO})_2)] \cdot x\text{H}_2\text{O}$ ($x \approx 1.3$)

The compound (II) consists of eight formula units in a c -centered monoclinic unit cell (see Figure 4). The structure is comprised of two crystallographically different ammonium ions, one lying on a two-fold axis and the other on a centre of symmetry, both having half multiplicity, and a vanadium based anion which are held together by both electrostatic forces and extensive hydrogen bonding. The vanadium atom environment is a seven

coordinate distorted pentagonal-bipyramid, with a vanadyl oxygen atom and a water molecule at the apices, and the peroxy group, the nitrogen atom from the pyridine ring and one oxygen atom from each carboxylate group forming an approximate pentagonal plane. Thus, the coordination geometry in the $[\text{VO}(\text{O}_2)(\text{H}_2\text{O})(\text{C}_5\text{H}_3\text{N}(\text{COO})_2)]^\ominus$ anion is similar to that observed in the $[\text{O}(\text{Ti}(\text{O}_2)(\text{H}_2\text{O})(\text{C}_5\text{H}_3\text{N}(\text{COO})_2))_2]^{2\ominus}$ anion²⁷, and is comparable to the seven coordination observed in other vanadium complexes, e.g. $(\text{NH}_4)_4[\text{O}(\text{VO}(\text{O}_2)_2)_2]^{5-}$ and $[\text{VO}(\text{NO}_3)_3 \cdot \text{CH}_3\text{CN}]^{43}$.

The vanadium atom is displaced 0.25Å out of the pentagonal plane towards the vanadyl oxygen atom O(1), which is closely comparable to the already mentioned displacements observed for other pentagonal-bipyramidal complexes. Again this observation can be attributed⁴² to the repulsions which result between the vanadium-oxygen π -bonding and the σ -bonds of the equatorial plane. In the $[\text{O}(\text{Ti}(\text{O}_2)(\text{H}_2\text{O})(\text{C}_5\text{H}_3\text{N}(\text{COO})_2))_2]^{2\ominus}$ anion²⁷, the titanium atom is coplanar with the pentagonal equatorial plane, as one might expect, since there are no titanium-oxygen π -bonds to cause a repulsion of the type described for the vanadium compound.

The V-O(1) bond length of 1.579(2)Å is significantly shorter than the V=O bond length of 1.606(3)Å observed in compound (I). Similarly, the V-O_{peroxy} bond lengths of 1.870(2) and 1.872(2)Å, and V-N(1) distance of 2.088(2)Å are also significantly shorter than the respective bond lengths of 1.882(3), 1.883(3) and 2.110(4)Å observed for (I). The effect expected in going from pentagonal-

pyramidal to pentagonal-bipyramidal coordination geometry would be a decrease in the corresponding nonbonded contact distances and an increase in the corresponding bonded distances to relieve steric crowding around the central vanadium atom. Instead of this, however, both the bond lengths and nonbonded contacts were observed to decrease. This systematic difference in the bond lengths must therefore be attributable to other factors. The problem is that these "other factors" are not easily defined. It has been suggested recently^{52,53} that collection of a limited sphere of data will result in a systematic shortening of bond lengths. The evidence for this appears to be exceedingly weak and is certainly of a smaller magnitude than that due to thermal motion. In addition, since the smallest d-spacing in this structure is 0.93Å **, then one might expect that any bond lengths longer than this value would show random rather than systematic variation. Secondly, the vanadyl oxygen atom in the anion of (I) was involved in a hydrogen bond, whereas O(1) in the anion of compound (II) has no hydrogen bonds, which could possibly account for the differences in the V=O bond lengths. On the other hand, the peroxo oxygens of both structures are involved in hydrogen bonding to approximately the same extent. Finally, it is possible that the dipicolinate ligand in the anion of (II) could withdraw electron density from the

**Calculated from the equation $\lambda = 2d\sin\theta_{max}$.

vanadium atom to the extent that a contraction of the bonds would occur. On this basis, one would expect a shorter O-O bond length for the peroxy group, as was observed. The mean V-O_{peroxy} bond lengths of 1.87Å, observed in (NH₄)₄[O(VO(O₂)₂)₂]⁵, and 1.89Å, observed in (NH₄)₃[V(O₂)₄]⁵, can only be said to be comparable to those in this structure.

The O(2)-O(3) bond length of 1.441(3)Å is significantly shorter than the peroxy bond length of 1.472(4)Å observed for (I) and is consistent with the stronger V-O_{peroxy} bonds in this structure. The mean O-O bond length of 1.44(3)Å observed for the compound (NH₄)₄[O(VO(O₂)₂)₂]⁵ is again comparable. As was the case for (I), shortening of the O-O bond can be attributed^{1,46,47} to the mode of coordination of the peroxy group. However, an alternative description^{1,46,47,51,54,55} of the peroxy group as a π-bonded monodentate ligand, and the coordination geometry around the metal atom as that of a distorted octahedron²⁷ would also explain these conclusions. In this latter description, the large deviations of the angles O(5)-V-N(1) (74.5(1)°) and O(7)-V-N(1) (74.3(1)°) from 90° would be expected as a result of steric interaction with the peroxy group.

Comparison of the pyridine-2,6-dicarboxylate ligand geometry in this structure to that observed in the [O(Ti(O₂)(H₂O)(C₅H₃N(COO)₂))₂]^{2⊖} anion²⁷ shows as a major difference the torsion angles that the carboxylate groups make with the pyridine ring. In this structure the carboxylate groups are out of

the plane of the pyridine ring by 1.4° and 5.7° , compared with 3.8° and 9.6° . Table XI compares the corresponding bond lengths and angles of (II) with $K_2[O(Ti(O_2)(H_2O)(C_5H_3N(COO)_2))_2].3H_2O$ ²⁷, dipicolinic acid⁵⁶, calcium dipicolinate⁵⁷, and strontium dipicolinate⁵⁸. Except for the inward bending distortion of the angles C(1)-C(2)-N(1) ($111.5(3)^\circ$), C(7)-C(6)-N(1) ($111.7(3)^\circ$), C(2)-C(1)-O(5) ($114.1(3)^\circ$), and C(6)-C(7)-O(7) ($113.3(3)^\circ$), and the corresponding outward bending angles, from 120° , the dimensions of the coordinated pyridine-2,6-dicarboxylate ligand are very comparable to those of the uncoordinated species. In addition, there are no significant differences observed between chemically equivalent bonds. Examination of the distances involving the titanium atom in the $[O(Ti(O_2)(H_2O)(C_5H_3N(COO)_2))_2]^{2\ominus}$ anion²⁷ indicate that on the average they are slightly longer than the corresponding bond distances in this structure. This would be consistent with the expectation that Ti(IV) has a larger covalent radius than V(V), since the latter has a higher nuclear charge, but the same electronic configuration, and from this one might predict a slightly longer peroxo bond length in the titanium complex, which appears to be the case, i.e. $1.45(1)\text{\AA}$ is slightly, but not significantly, longer.

The mean C-H, N-H, and O-H bond lengths observed in this structure are comparable to those observed for the compound $Cr(CO_2CH_2NH_2)_3.H_2O$ ⁵⁰, i.e. 0.96 , 0.81 , and 0.80\AA compared to $0.96(5)$, $0.88(4)$, and $0.88(4)\text{\AA}$, respectively.

Table XI : Comparison Between The Corresponding Bond Lengths (Å)
And Angles (Deg.) For The Compounds
 $\text{NH}_4[\text{VO}(\text{O}_2)(\text{H}_2\text{O})(\text{C}_5\text{H}_3\text{N}(\text{COO})_2)] \cdot x\text{H}_2\text{O}$ ($x \approx 1.3$) (A),
 $\text{K}_2[\text{O}(\text{Ti}(\text{O}_2)(\text{H}_2\text{O})(\text{C}_5\text{H}_3\text{N}(\text{COO})_2))_2] \cdot 3\text{H}_2\text{O}$ (B),
Dipicolinic Acid (C), Calcium Dipicolinate (D),
And Strontium Dipicolinate (E).

(a) Bond Lengths:

Bonds	(A)	(B)	(C)	(D)	(E)
N(1)-C(2)	1.327	1.36	1.338	1.339	1.335
N(1)-C(6)	1.325	1.32	1.336	1.326	1.335
C(1)-O(5)	1.280	1.27	1.288	1.256	1.258
C(1)-O(6)	1.233	1.23	1.217	1.240	1.245
C(1)-C(2)	1.498	1.49	1.507	1.500	1.525
C(2)-C(3)	1.384	1.38	1.399	1.395	1.381
C(3)-C(4)	1.388	1.44	1.372	1.395	1.385
C(4)-C(5)	1.380	1.43	1.378	1.374	1.385
C(5)-C(6)	1.378	1.40	1.388	1.379	1.381
C(6)-C(7)	1.505	1.50	1.511	1.508	1.525
C(7)-O(7)	1.288	1.28	1.315	1.254	1.245
C(7)-O(8)	1.223	1.22	1.181	1.245	1.258

...cont'd

Table XI : cont'd

(b) Bond Angles:

Angles	(A)	(B)	(C)	(D)	(E)
C(6)-N(1)-C(2)	121.8	122	116.8	119.6	118.8
N(1)-C(2)-C(3)	120.8	122	123.4	122.4	122.4
C(2)-C(3)-C(4)	117.8	117	118.9	116.9	118.7
C(3)-C(4)-C(5)	120.4	120	118.2	120.1	118.9
C(4)-C(5)-C(6)	118.2	118	119.4	119.0	118.7
C(5)-C(6)-N(1)	120.9	121	123.3	121.6	122.4
N(1)-C(2)-C(1)	111.5	111	118.4	114.9	115.4
C(3)-C(2)-C(1)	127.7	127	118.2	122.7	122.4
N(1)-C(6)-C(7)	111.7	111	115.3	114.8	115.4
C(5)-C(6)-C(7)	127.4	128	121.4	123.3	122.4
C(2)-C(1)-O(6)	120.5	119	119.2	117.6	117.4
C(2)-C(1)-O(5)	114.1	114	116.3	116.9	117.2
O(5)-C(1)-O(6)	125.4	127	124.4	125.4	125.5
C(6)-C(7)-O(8)	120.7	118	124.8	116.4	117.2
C(6)-C(7)-O(7)	113.3	114	110.8	118.1	117.4
O(7)-C(7)-O(8)	126.0	128	124.4	125.5	125.3

The constituent ions and water molecules of complex(II) are arranged in alternating organic and inorganic 'layers' normal to the b-axis, i.e. the anions are arranged such that the peroxy groups are always adjacent to one another, as are the pyridine rings (see Figure 4). This is similar to what was found in the complex $K_2[O(Ti(O_2)(H_2O)(C_5H_3N(COO)_2))_2].3H_2O$ ²⁷. The ammonium ions are located in holes in the inorganic layers, with all nearest neighbours being oxygen atoms, and are involved, along with the water molecules, in extensive hydrogen bonding. The organic layers have only van der Waals forces to hold the structure together. Almost all of the contacts between nonhydrogen atoms, which are less than 3.2Å, represent hydrogen bonds, as indicated by the interionic/intermolecular distances and angles given in Table VII.

4.3. Sequel.

The results from the structural study of (I) have already been published⁵⁹. In addition, the results from the structural study of (II) were presented at the Ninth General Assembly And International Congress of the International Union Of Crystallography⁶⁰ which was held in Kyoto, Japan in the Fall of 1972. These results have also been accepted for publication⁶¹.

APPENDIX A

COMPUTATIONS AND COMPUTER PROGRAMS UTILIZED FOR THE DETERMINATION AND ANALYSIS OF THE CRYSTAL STRUCTURES

The following describes only those features of the various programs that were actually used.

A.1. DATAPR - A Data Reduction Program.

A program to convert the intensity data obtained during the data collection into structure factor amplitudes $|F_{hkl}|$, applying both Lorentz (L) and polarization (p) corrections.

The Lorentz factor is concerned with the time required for a reciprocal lattice point to pass through the sphere of reflection. It varies with the geometries of different experiments, but for diffractometer data collected by the θ - 2θ scan technique, it is given by:

$$L = (\sin 2\theta)^{-1} \quad (A1)$$

The polarization term arises from a reduction of the scattered intensity due to polarization effects of electromagnetic radiation upon reflection and depends on the angle θ . If the incident beam is unpolarized, it is given by:

$$p = \frac{1}{2}(1 + \cos^2 2\theta) \quad (A2)$$

For a unit cell containing N atoms, the structure factor (F) is a function of the fractional coordinates (x_n, y_n, z_n) , the scattering factor (f_n) and the temperature factor (B_n) of the nth atom, as well as the Miller Indices (h,k,l) :

$$F_{hkl} = \sum_{n=1}^N f_n e^{-B_n \sin^2 \theta / \lambda^2} e^{[2\pi i(hx_n + ky_n + lz_n)]} \quad (A3)$$

where f_n in general can be written as the sum of the Rayleigh scattering (f_o), which is the dominant factor, and the real ($\Delta f'$) and imaginary ($\Delta f''$) terms due to anomalous scattering:

$$f_n = f_o + \Delta f' + i\Delta f'' \quad (A4)$$

To find the atomic positions, one must be able to relate the structure factor (F) to the measured intensity (I_{obs}), which is the expression:

$$|F_{hkl}| = \sqrt{\frac{KI_{obs}A}{Lp}} = |F_{obs}| \quad (A5)$$

where K is a constant known as the scale factor, and A is the absorption term. The constant K is determined by the crystal size, the beam intensity, and variations during data collection. The absorption term A is difficult to calculate exactly as it requires a precise description of the crystal shape, but as mentioned in chapter 2, it was possible to neglect this term.

The output from this program included generation of the BUFILE for input into the program BUCILS, and a listing of the observed $|F_{hkl}|$, $|F_{hkl}|^2$, $|F_{hkl}|^2/Lp$ and the net count for each reflection. The original program was written by F.R.Ahmed, for the National Research Council of Canada, and has been further modified at S.F.U.

A.2. FORDAP - A Program to Calculate Fourier Syntheses.

This program for computing Fourier syntheses was utilized for the calculation of the Patterson function based on $|F_{obs}|^2$, obtained from the BUCFILE, and the Fourier electron density syntheses and difference syntheses which were based on the signed F_{obs} and F_{calc} , obtained from the FORFILE.

The Patterson function of an electron density distribution:

$$\rho(x,y,z) = \frac{1}{V} \sum_{hkl} F_{hkl} \exp[-2\pi i(hx + ky + lz)] \quad (A6)$$

is defined⁶² to be:

$$P(u,v,w) = \int_0^1 \int_0^1 \int_0^1 \rho(x,y,z) \rho(x+u,y+v,z+w) V dx dy dz \quad (A7)$$

or represented by the Fourier series:

$$P(u,v,w) = \frac{1}{V} \sum_{hkl} |F_{hkl}|^2 \exp[2\pi i(hu + kv + lw)] \quad (A8)$$

The physical significance of (A7) is that $P(u,v,w)$ is only much greater than zero for those values of (u,v,w) that represent electron density overlap. For a set of N atoms, the Patterson function contains N^2 peaks, N of these coincide to form the origin peak. One-half of the remaining peaks, i.e. $N(N-1)/2$, are related to the other half by a centre of symmetry. The weight of a peak in a Patterson map is proportional to the product of the atomic numbers of the two atoms involved. Peaks generated by the heavy atoms are therefore most prominent in the map, and a set of chemically reasonable atomic coordinates can be worked out to fit these major features.

Equation (A6) gives the electron density distribution in a Fourier series representation. The coefficient F's for the first Fourier electron density map can be obtained by two methods. Direct Methods yield a set of phased E's which give the phases of the corresponding F's whose amplitudes are obtained from (A5). Although the summation is not over the entire set of hkl values measured, the electron density map will give initial atomic positions since the input F's are always large in their respective ranges of $(\sin\theta)/\lambda$. The other method is the solution of the Patterson function to obtain a set of atomic coordinates from which approximate $F_{o.a.1o}$'s can be computed using equation (A3) and some assumed or predetermined temperature factors. If the heavy atoms represent a high percentage of the scattering material, and if none or only some of the light atom positions are recovered from the Patterson map, then the coordinates of the heavy atoms should be sufficient to constitute an initial phasing model even though the summation of (A3) is not over the entire contents of the unit cell.

If the quantities $\Delta F = F_{o.b.s} - F_{o.a.1o}$, where $F_{o.b.s}$ takes the phase of the corresponding $F_{o.a.1o}$, are used as coefficients in the Fourier series, an electron density difference map is obtained. As suggested by the definition of ΔF , the map will reveal the difference between the true structure and the model used. It is therefore useful in locating light atoms, correcting misplaced atoms and detecting anisotropic thermal motion.

The program FORDAP was written by Dr. A.Zalkin, at the University of California, and has options for computing either Patterson, electron density or difference syntheses. Output is in the form of a three-dimensional electron density map and lists of the most intense peaks and troughs on the map.

A.3. SAP - A Set Of Programs For Symbolic Addition Procedures.

This is a set of direct phasing programs for solving structures by the Symbolic Addition Procedure^{s3}, and was written by S.Hall and F.R.Ahmed of the National Research Council of Canada.

The normalized structure factors (E's) are obtained from the relationship:

$$|E_{hkl}| = \sqrt{\frac{|F_{hkl}|^2}{\mathcal{E} \sum_1^n f_1^2}} \quad (A9)$$

where \mathcal{E} is an integer which is generally 1, but may assume other values for special sets of reflections in certain space groups. The distribution of the $|E|$ values is independent of the size and content of the unit cell, but does depend on the presence or absence of a centre of symmetry in the space group. As a result, the distribution of the $|E|$ values can be utilized as a statistical test for centric and acentric distributions of intensities.

For centrosymmetric structures, as was (II), this program makes use of one of the most powerful and widely used relationships, the Σ_2 principle:

$$\text{sign}(E_h) \approx \text{sign}(\sum_{k_r} E_k E_{h-k}) \quad (\text{A10})$$

where E_h is the normalized structure factor of the reflection h , and k_r implies the k ranges only over high $|E|$ reflections. The symbol \approx means "is probably equal to". The probability⁶⁴ that the Σ_2 relationship is true is equal to:

$$P \approx \frac{1}{2} + \frac{1}{2} \tanh\{\sigma_3 \sigma_2^{3/2} |E_h E_k E_{h-k}|\} \quad (\text{A11})$$

where $\sigma_3 = \sum_1 Z_1^3$ and $\sigma_2 = \sum_1 Z_1^2$, summation being over the unit cell and Z_1 being the atomic number of atom 1.

The SAP programs give tentative signs to the E's of the Σ_2 triplets when the product sum accumulated is higher than a test limit. Reflections with acceptable tentative signs are then included in the list of signed reflections and are used in turn. The test limit values are lowered successively to generate more tentative signs. This ensures that only highly probable correct signs are included in the early stages of sign development. When the minimum test limit is reached and there are still reflexions with undetermined signs, a symbol is assigned to the reflection that has the most triplets among the first ten highest E's. The whole process is repeated with the first test limit and so on. More symbols can be assigned if necessary, to a maximum of four. The program then seeks for consistent indication to determine the actual signs of the symbols and their products.

A.4. BUCILS - A Program For Calculating Structure Factors
And Full-Matrix Least-Squares Refinement.

This is a program for the calculation of structure factors and the full-matrix least-squares refinement of the scale, atomic positional and thermal parameters in the structures. It was based on the program UCILS written at Northern University and the University of California at Irvine, and has been modified both at the University of Canterbury (N.Z.) and S.F.U. The observed structure factors are input via the BUCFILE (see A.1. above).

After a trial phasing model is obtained, refinement of the scale (k') between the observed and calculated structure factors, and the positional as well as thermal parameters of the atoms is by full-matrix least-squares methods⁶⁵. The quantity minimized was:

$$D = \sum_{hkl} w_{hkl} (|F_{r.o.}| - k'|F_{c.a.l.}|)^2 \equiv \sum_{hkl} w_{hkl} \Delta^2 \quad (A12)$$

where w_{hkl} are the weights, and

$$|F_{r.o.}| = k'|F_{o.b.s}| = \sqrt{I_{o.b.s} A / Lp} \quad (A13)$$

The functional form of the structure factor is nonlinear, therefore it has to be approximated by a truncated Taylor series. The refined values of the parameters from a cycle of least-squares procedure are only better approximations to their best values than those before refinement. Calculations must therefore be repeated until the iterative process produces no significant change in the parameters.

BUCILS was used to write the following files:

FORFILE - contained calculated and observed structure factor information for use in the program FORDAP and for analysis of R factors and weights by program RANGER;

ORFFILE - contained atomic coordinates, temperature factors, standard deviations and the correlation matrix of the least-squares refinement for program ORFFE2.

Output from BUCILS could include the scale, atomic coordinates and thermal parameters based on any or all of the cycles of least-squares refinement; the shifts in the parameters from the previous cycle; the correlations between the various parameters and the residual index, R.

A.5. RANGER - A Program For Analysis Of R Factors And Weights.

A program to analyze R factors and weights for different classes of reflections based on $|F_{obs}|$, $\sin\theta$ or indices. This program was originally written by Dr.P.W.R.Corfield at Northwestern University and modified at the University of Canterbury (N.Z.) and S.F.U. Input data is from the FORFILE.

A.6. DANFIG - A Program For Calculating Interatomic Distances And Angles.

A program for calculation of interatomic distances and angles based on a program by W.H.Baur and modified at the University of Canterbury (N.Z.) and S.F.U. Input included the atomic positional

and thermal parameters obtained from BUCILS and/or FORDAP. Output listed all atoms closer than a specified distance from all other atoms and listed the contact angles around each atom.

A.7. ORFFE2 - A Program For Calculating Interatomic Distances
And Angles With Standard Deviations.

A program to calculate interatomic distances and angles with standard deviations, to calculate the root-mean-square component of thermal motion along various axes and to calculate interatomic distances averaged over thermal motion. The program used was a modified version of the program written by W.R.Busing, K.O.Martin and H.A.Levy at the Oak Ridge National Laboratory. Input of information is via the ORFFILE.

A.8. MEANPLANE - A Program For Calculating Mean Planes.

A program to calculate least-squares mean planes through various groups of atoms and the deviations of the atoms from that plane. This program was originally written by M.E.Pippy and F.R.Ahmed for the National Research Council of Canada and has been modified at S.F.U. Input includes atomic coordinates with their estimated standard deviations and the unit cell dimensions. Output lists the coefficients from the equation for the plane:

$$Ax + By + Cz + D = 0 \quad , \quad (A14)$$

the χ^2 value as an indication of the planarity of the plane, the distance of each atom from the plane, and the angles between the plane and all other planes defined.

A.9. ORTEP - A Program For Crystal Structure Illustrations.

A program to plot thermal-ellipsoids and/or spheres, via a Calcomp plotter, for crystal structure illustrations, using the atomic coordinates and thermal parameters, and the unit cell dimensions. The program was written by C.K.Johnson of the Oak Ridge National Laboratory, Oak Ridge, Tennessee (U.S.A.) and modified at S.F.U.

A.10. MGTLS - A Rigid-Body Analysis Program.

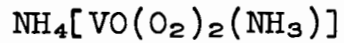
A program to calculate translational, librational and screw tensors for a molecule or ion and to correct these thermal motion effects on the bond lengths which result from the group moving as a rigid-body. The program was written by K.N.Trueblood. Input includes the atomic weights, the atomic coordinates and the thermal parameters.

A.11. FILIST - A Program For Listing Structure Factors.

A program which lists the calculated and observed structure factors, for all of the reflections measured, in a format suitable for the preparation of the tables for publication. This program is based on a program from the University of Canterbury, New Zealand.

APPENDIX B

THE MEASURED AND CALCULATED STRUCTURE FACTORS FOR



The measured and calculated structure factors for the complex $\text{NH}_4[\text{VO}(\text{O}_2)_2(\text{NH}_3)]$ are presented below. The unobserved reflections have a value of $\sigma/2$ and are denoted by a negative value of F_{obs} .

085	C/LC	8	3	-35	31	3	1	368	-368	4	11	-37	-27	0	9	-26	26	6	7	-26	23	3	7	141	-136	5	6	59	51	0	9	96	-104	5	2	-32	4		
0	0	4	3	-37	35	4	1	206	-206	0	12	-64	64	0	10	81	93	7	7	81	-83	4	7	97	-100	7	6	-82	-51	1	9	91	81	0	2	-40	-33		
0	4	451	449	3	1	401	398	1	12	-63	66	2	10	178	-178	0	0	131	190	3	7	205	194	0	7	69	96	0	7	69	96	0	3	-32	14				
0	4	133	-126	6	4	1	66	-90	2	12	-37	-21	3	10	92	-87	0	8	-29	-18	0	8	81	-72	1	7	-35	-37	0	10	74	70	2	3	113	106			
0	4	261	-249	6	7	1	206	-213	3	12	-43	-32	2	10	118	120	3	8	-34	39	0	8	149	143	2	7	-36	-44	1	10	137	141	4	3	66	-49			
602	-569	3	4	78	72	8	1	74	-40					5	10	-35	33	4	8	-37	33	1	8	139	125	4	7	-42	37	2	10	135	-133	0	4	-35	9		
1071	1098	4	4	243	243	9	1	111	114					1	11	-157	158	5	8	-33	-2	2	8	192	-191	5	7	-38	-33										
300	-267	5	4	62	-64	0	2	932	940					1	11	-177	179	0	9	-28	7	5	8	126	126	0	8	106	-106										
993	-932	6	4	142	-129	1	2	370	-371					2	11	-41	-49	0	9	-28	84	4	8	125	126	0	8	106	-106										
516	510	7	4	-33	3	2	2	370	-371					2	11	-41	-49	0	9	-28	84	4	8	125	126	0	8	106	-106										
444	-436	8	4	112	103	3	2	-25	-10	0	1	1	108	-162																									
264	255	9	4	-35	-14	4	2	544	543	2	1	107	107	0	10	124	-122	2	9	-34	31	0	8	123	-116	2	8	82	84	0	0	157	158	3	4	-44	-72		
1142	-1132	0	5	239	248	5	2	-30	-33	5	2	-124	-125	4	1	92	-90	1	12	-35	-32	2	9	112	114	0	9	-35	29	1	0	125	-126	5	4	-63	61		
49	41	1	5	309	-316	6	2	193	-192	4	1	92	-90	1	12	-35	-32	2	9	-37	-40	0	9	119	-128	5	8	-39	-47	1	10	137	141	4	3	66	-49		
660	-661	2	5	63	-62	7	2	-35	-42	5	1	93	-93	2	12	143	149	5	9	-33	-28	2	0	96	-93	4	8	-34	-26	3	0	144	-145	0	5	126	127		
123	122	3	5	270	270	8	2	169	162	6	1	-31	-31	15	0	0	0	0	10	-32	9	4	9	101	-101	1	9	-39	60	5	0	199	200	2	5	136	-131		
211	-207	4	5	118	121	9	2	-32	-13	7	1	-30	-17	0	10	-33	4	5	0	101	-101	1	9	101	-101	1	9	-39	60	5	0	199	200	2	5	136	-131		
430	436	5	5	254	-250	0	3	478	470	8	1	-36	-19	0	10	-33	4	5	0	101	-101	1	9	101	-101	1	9	-39	60	5	0	199	200	2	5	136	-131		
654	-662	6	5	-32	-36	1	3	386	-368	9	1	-35	15	0	10	-37	-40	0	10	99	-95	2	9	101	-101	1	9	-39	60	5	0	199	200	2	5	136	-131		
191	195	7	5	-180	173	2	3	81	72	0	2	624	-612	0	0	383	383	3	10	-33	-9	1	10	-37	-44	3	9	-37	-16	1	1	206	-206	5	5	-16	-17		
229	-229	8	5	-39	43	3	3	555	559	1	2	40	-43	1	0	195	184	3	10	-34	-1	2	10	211	209	0	10	-37	23	2	1	202	-209	0	5	111	-106		
97	97	0	6	666	-643	4	3	234	233	2	2	50	-58	3	0	126	-127	5	10	-31	-1	3	10	-63	66	1	10	-36	-4	3	1	126	126	1	6	211	-196		
243	291	1	6	59	-54	5	3	197	-156	3	2	85	-89	4	0	126	129	0	11	-33	-3	4	10	109	-110	1	10	-37	-4	4	1	105	101	2	6	-37	37		
398	391	3	6	55	55	7	3	203	164	5	2	-28	-24	5	0	109	113	2	11	-34	-25	1	11	94	93	1	11	-34	-25	1	1	135	-140	3	6	138	135		
-32	-29	4	6	301	-297	8	3	81	86	6	2	-34	-39	6	0	219	-232	3	11	-34	-6	2	11	94	93	1	11	-34	-25	0	0	1	1	135	-140	3	6	138	135
191	176	5	6	-31	-26	9	2	99	-93	7	2	-35	-38	4	0	43	55	4	11	-32	-7	3	11	104	-111	1	11	-32	-7	0	0	1	1	135	-140	3	6	138	135
332	-344	6	6	182	174	0	4	375	-384	8	2	-33	-39	9	0	-37	20	1	12	-33	3	11	104	-111	1	11	-32	-7	0	0	1	1	135	-140	3	6	138	135	
485	484	7	6	-35	-27	1	5	182	-111	9	2	-31	-2	9	0	-37	20	1	12	-33	3	11	104	-111	1	11	-32	-7	0	0	1	1	135	-140	3	6	138	135	
132	-129	8	6	102	-97	2	4	529	535	0	3	79	68	1	1	831	831	1	12	-33	3	11	104	-111	1	11	-32	-7	0	0	1	1	135	-140	3	6	138	135	
208	198	9	7	207	-208	3	4	201	202	1	3	201	-221	1	1	468	-470	1	12	-33	3	11	104	-111	1	11	-32	-7	0	0	1	1	135	-140	3	6	138	135	
193	-192	1	7	335	338	4	4	410	-407	2	3	-25	-26	3	1	179	182	3	12	-33	3	11	104	-111	1	11	-32	-7	0	0	1	1	135	-140	3	6	138	135	
-28	-19	2	8	118	117	6	3	-30	24	4	2	76	-81	2	0	200	-212	4	12	-34	-1	2	10	211	209	0	10	-37	23	2	1	202	-209	0	5	111	-106		
155	-152	3	7	194	-200	6	4	133	133	4	3	74	76	3	1	418	422	0	1	-23	-19	0	0	494	-498	6	1	81	83	0	2	122	-125	5	2	126	-125		
-40	39	4	7	108	-121	7	4	92	78	5	3	79	-80	5	1	315	-317	0	1	72	-60	4	0	204	195	3	1	-37	20	1	3	67	74						
88	-90	5	7	229	234	8	4	193	-186	6	3	-60	-67	7	1	114	119	2	1	101	-102	4	0	204	195	3	1	-37	20	1	3	67	74						
61	34	6	7	-33	35	9	4	-31	-26	7	3	119	116	8	1	114	119	2	1	101	-102	4	0	204	195	3	1	-37	20	1	3	67	74						
-32	-34	7	7	137	-125	0	5	474	-462	9	3	-38	-39	8	1	123	136	3	1	85	99	5	0	204	195	3	1	-37	20	1	3	67	74						
-34	33	8	7	40	-40	1	5	220	228	9	3	68	-64	9	1	114	-105	5	1	43	22	7	0	74	95	7	1	-40	-36	5	4	3	39	54					
-39	-36	0	8	323	331	2	5	179	-183	0	4	181	-183	0	1	114	-105	5	1	43	22	7	0	74	95	7	1	-40	-36	5	4	3	39	54					
339	330	1	8	-31	-33	3	5	363	-367	1	4	71	-74	2	2	417	-411	0	1	-32	5	0	0	349	-350	1	2	179	-177	1	1	127	126	4	0	-37	-24		
332	-344	2	9	254	-251	4	6	349	342	7	4	63	58	2	2	554	556	1	1	-37	21	1	1	399	-401	6	2	-46	-40	4	0	104	103	3	1	134	-133		
159	150	3	8	-30	-36	5																																	

APPENDIX C

THE MEASURED AND CALCULATED STRUCTURE FACTORS FOR $\text{NH}_4[\text{VO}(\text{O}_2)(\text{H}_2\text{O})(\text{C}_5\text{H}_3\text{N}(\text{COO})_2)] \cdot x\text{H}_2\text{O}$ ($x \approx 1.3$)

The measured and calculated structure factors for the complex $\text{NH}_4[\text{VO}(\text{O}_2)(\text{H}_2\text{O})(\text{C}_5\text{H}_3\text{N}(\text{COO})_2)] \cdot x\text{H}_2\text{O}$ ($x \approx 1.3$) are presented below. The unobserved reflections have a value of $\sigma/2$ and are denoted by an asterisk after the value of F_{obs} .

REFERENCES .

- (1) J.A.Connor and E.A.Ebsworth;
Advan. Inorg. Chem. Radiochem., 6 , 279 (1964).
- (2) J.F.Fergusson, C.J.Wilkins and J.F.Young;
J. Chem. Soc., 2136 (1962).
- (3) R.Stomberg; Acta Chem. Scand., 17 , 1563 (1963).
- (4) G.Mathern and R.Weiss;
Acta Crystallogr., B27 , 1598 (1971).
- (5) I-B.Svensson and R.Stomberg;
Acta Chem. Scand., 25 , 898 (1971).
- (6) J.Sala-Pala and J.E.Guerchais;
J. Chem. Soc.(A), 1132 (1971).
- (7) G.Mathern and R.Weiss;
Acta Crystallogr., B27 , 1582 (1971).
- (8) G.Mathern and R.Weiss;
Acta Crystallogr., B27 , 1572 (1971).
- (9) R.Stomberg; Acta Chem. Scand., 22 , 1076 (1968).
- (10) A.Mitschler, J.M.LeCarpentier and R.Weiss;
Chem. Commun., 1260 (1968).
- (11) R.Weiss, J.M.LeCarpentier, A.Mitschler and R.Schlupp;
Acta Crystallogr., A25(Supp.) , 171 (1969).
- (12) F.W.B.Einstein and B.R.Penfold;
Acta Crystallogr., 17,1127 (1964).
- (13) R.Stomberg; Arkiv Kemi, 22 , 29 (1964).
- (14) R.Stomberg and I.B.Ainalem;
Acta Chem. Scand., 22 , 1439 (1968).

- (15) R.Stomberg; Arkiv Kemi, 24 , 111 (1965).
- (16) F.J.C.Rossotti and H.Rossotti;
Acta Chem. Scand., 10 , 957 (1956).
- (17) N.Ingro and F.Brito;
Acta Chem. Scand., 13 , 1971 (1959).
- (18) O.W.Howarth and R.E.Richards;
J. Chem. Soc., 864 (1965).
- (19) G.A.Dean; Can. J. Chem., 39 , 1174 (1961).
- (20) M.Orhanovic and R.G.Wilkins;
J. Amer. Chem. Soc., 89 , 278 (1967).
- (21) P.Souchay and F.Chauveau;
Compt. rend., 245 , 1434 (1957).
- (22) K.F.Jahr, L.Schoepp and J.Fuchs;
Z. Naturforsch, 14b , 469 (1959).
- (23) G.Kakabadse and H.J.Wilson;
J. Chem. Soc., 2475 (1960).
- (24) P.Melikov and L.Pissarevski;
Z. Anorg. Chem., 19 , 405 (1898).
- (25) H.Hartkamp; Angew. Chem., 71 , 553 (1959).
- (26) H.Hartkamp; Z. Anal. Chem., 171 , 262 (1959).
- (27) D.Schwarzenbach; Inorg. Chem., 9 , 2391 (1970).
- (28) L.A.Frolova, G.A.Bogdanov and G.K.Yurchenko;
Zh. Fiz. Khim., 40 , 1592 (1966).
- (29) H.J.Emeleus and J.S.Anderson;
"Modern Aspects Of Inorganic Chemistry",
Routledge and Kegan Paul Ltd., London (1963), p.425 .

- (30) R.E.Drew and F.W.B.Einstein; unpublished results.
- (31) R.D.Burbank; Acta Crystallogr., 19 , 957 (1965).
- (32) P.Coppens; Acta Crystallogr., A24 , 253 (1968).
- (33) A.M.O'Connell, A.I.M.Rae and E.N.Maslen;
Acta Crystallogr., 21 , 208 (1966).
- (34) "International Tables Of X-Ray Crystallography";
Vol.III, Kynoch Press, Birmingham, England (1965), Section 3.3 .
- (35) R.F.Stewart, E.R.Davidson and W.T.Simpson;
J. Chem. Phys., 42 , 3175 (1965).
- (36) V.Schomaker and K.N.Trueblood;
Acta Crystallogr., B24 , 63 (1968).
- (37) J.Karle and I.L.Karle;
Acta Crystallogr., 21 , 849 (1966).
- (38) D.Sayre; Acta Crystallogr., 5 , 60 (1952).
- (39) D.Harker and J.S.Kasper;
Acta Crystallogr., 1 , 70 (1948).
- (40)(a) W.C.Hamilton and J.A.Ibers;
"Hydrogen Bonding In Solids",
W.A.Benjamin, New York, N.Y. (1968), p.64 .
- (b) W.C.Hamilton; "Statistics In Physical Science",
The Ronald Press Co., New York, N.Y. (1964), p.157-162.
- (41) C.N.Caughlan, H.M.Smith and K.Watenpaugh;
Inorg. Chem., 5 , 2131 (1966).
- (42) R.J.Gillespie and R.S.Nyholm;
Quart. Rev. Chem. Soc., 11 , 339 (1957).
- (43) F.W.B.Einstein, E.Enwall, D.M.Morris and D.Sutton;
Inorg. Chem., 10 , 678 (1971).

- (44) K.J.Palmer; J. Amer. Chem. Soc., 50 , 2360 (1938).
- (45) D.Bruins and D.I.Weaver; Inorg. Chem., 5 , 2131 (1966).
- (46) R.Stomberg; Arkiv Kemi, 24 , 283 (1965).
- (47) D.M.P.Mingos; Nature(London), 230 , 154 (1971).
- (48) J.C.Evans; Chem. Commun., 682 (1969).
- (49) W.P.Griffith; J. Chem. Soc., 3949 (1962).
- (50) R.F.Bryan, P.T.Greene, P.F.Stokely and E.W.Wilson,Jr.;
Inorg. Chem., 10 , 1468 (1971).
- (51) D.G.Tuck and R.M.Walters;
Inorg. Chem., 2 , 428 (1963).
- (52) D.M.Collins and J.L.Hoard;
J. Amer. Chem. Soc., 92 , 3761 (1970).
- (53) W.R.Scheidt, R.Countryman and J.L.Hoard;
J. Amer. Chem. Soc., 93 , 3878 (1971).
- (54) J.A.McGinnety and J.A.Ibers;
Chem. Commun., 235 (1968).
- (55) R.Stomberg; Acta Chem. Scand., 22 , 1439 (1968).
- (56) F.Takusagawa, K.Hirotsu and A. Shimada; to be published.
- (57) G.Strahs and R.E.Dickerson;
Acta Crystallogr., B24 , 571 (1968).
- (58) K.J.Palmer, R.Y.Wong and J.C.Lewis;
Acta Crystallogr., B28 , 233 (1972).
- (59) R.E.Drew and F.W.B.Einstein;
Inorg. Chem., 11 , 1079 (1972).
- (60) R.E.Drew and F.W.B.Einstein;
Acta Crystallogr., A28 , Part S4 , S86 (1972).

- (61) R.E.Drew and F.W.B.Einstein;
Inorg. Chem., 12 , in press; expected to appear in the April
issue, 1973.
- (62) H.Lipson and W.Cochran; "The Crystalline State",
Vol.III, Sir Lawrence Bragg (Ed.), G.Bell and Sons Ltd.,
London, England (1966), Chapter 7.
- (63) F.R.Ahmed; "Crystallographic Computing",
F.R.Ahmed (Ed.), Munksgaard, Copenhagen, Denmark (1970), p.55 .
- (64) W.Cochran and M.M.Woolfson;
Acta Crystallogr., 8 , 1 (1965).
- (65) J.S.Rollet; "Computing Methods In Crystallography",
J.S.Rollet (Ed.), Pergamon Press, New York, N.Y. (1965), p.47 .